

THESIS FOR THE DEGREE OF DOCTOR OF PHILOSOPHY IN NATURAL SCIENCE,
SPECIALIZATION IN CHEMISTRY

**Secondary Organic Aerosols:
Composition, Gas-to-Particle Partitioning and Physical Properties**

Anna Ida Lutz



UNIVERSITY OF GOTHENBURG

Department of Chemistry and Molecular Biology
University of Gothenburg
SE-412 96 Gothenburg,
Sweden

Doctoral thesis submitted for fulfilment of the requirements for the degree of
Doctor of Philosophy in Natural Science, Specialization in Chemistry

Secondary Organic Aerosols: Composition, Gas-to-Particle Partitioning and Physical Properties

© Anna Ida Lutz, 2019

Cover photo: Aerosol formation over Hong Kong

Photo: Christian Mark Salvador

Atmospheric Science,
Department of Chemistry and Molecular Biology,
University of Gothenburg,
SE-412 96 Gothenburg,
Sweden

Printed by BrandFactory
Kållerød, Sweden

ISBN: 978-91-7833-362-2 (PRINT)

ISBN: 978-91-7833-363-9 (PDF)

<http://hdl.handle.net/2077/58699>

Abstract

Atmospheric aerosols influence our climate and air quality. Aerosol particles in the atmosphere are transformed through many different physical and chemical reactions. A substantial fraction of the particles in the atmosphere are of secondary origin, formed as a result of gas to particle conversion. The formation process of secondary organic aerosols (SOA) from oxidation of volatile organic compounds (VOC) is currently not fully understood. The objective of this thesis is to contribute to the understanding of factors important for secondary particle formation by simulating certain atmospheric processes in a flow reactor and by measurements of organic compounds in the ambient atmosphere. This work focuses on the formation of secondary organic particles via gas to particle conversion, their chemical composition and the volatility of the compounds. These factors are important for understanding the formation and evolution of secondary particles in the atmosphere, which in turn is important for making predictions about our future climate.

The chemical composition of SOA was studied using a chemical ionization high-resolution time-of-flight mass spectrometer connected to a Filter Inlet for Gases and Aerosols (FIGAERO-ToF-CIMS). The analysis was performed on samples from three sites: a boreal forest in Europe, a temperate forest in North America and a semi-urban location near a major city in Asia.

In order to model SOA and thus be able to predict its impact on society, in particular relating to climate change and health issues, accurate models for SOA formation are needed. The basis for such models includes understanding gas to particle partitioning and the factors that influence this partitioning. In addition, knowledge of the compounds in the particles is needed. The work revealed ways in which anthropogenic pollution could affect the partitioning and consequently the formation of SOA. It was shown that equilibrium phase partitioning behaves as predicted under some circumstances, such as when the air was not affected by anthropogenic pollution. However, when the air masses were affected by anthropogenic pollution, equilibrium phase partitioning does not behave as expected, due to restrictions in uptake and the aerosol not being in equilibrium. This effect was especially seen for highly oxygenated compounds.

Keywords: gas to particle conversion, volatility, secondary organic aerosols, FIGAERO, CIMS, monoterpenes, isoprene, SOA, BVOC.

Sammanfattning

Aerosoler i atmosfären påverkar vår luftkvalitet och vårt klimat. Aerosol-partiklarna påverkas av flera kemiska och fysikaliska processer i atmosfären. En stor andel av partiklarna i atmosfären är sekundära. Sekundära Organiska Aerosoler (SOA) bildas när flyktiga organiska ämnen (VOC) oxideras i atmosfären och det råder osäkerhet kring detaljerna kring hur detta går till. Målet med denna avhandling är att öka kunskapen om SOA och vilka faktorer som påverkar deras bildning. Detta har gjorts genom att simulera specifika atmosfäriska processer i ett flödesrör samt genom att mäta organiska ämnen i atmosfären. Fokus för denna avhandling är att studera hur gas till partikelomvandlingen som skapar SOA går till, vilka kemiska sammansättningar SOA har samt mäta SOA-partiklarnas flyktighet.

Den kemiska sammansättningen av SOA studerades med en masspektrometer som använder kemisk jonisering för att mäta organiska ämnen i gas- och partikelfas (FIGAERO-ToF-CIMS). Analyserna av aerosoler utomhus gjordes på tre mätstationer: en boreal skog i Europa, en skog i tempererat klimat i Nordamerika och i utkanten av en stor stad i Asien.

För att kunna modellera SOA, och därmed hur SOA påverkar vårt klimat och vår hälsa, behövs tillförlitliga modeller. Grunden för modellernas tillförlitlighet innefattar detaljerad kännedom om gas till partikelomvandling. Utöver det behövs kunskap om partiklarnas kemiska sammansättning. I denna avhandling klargörs även hur mänskliga utsläpp påverkar fasfördelningen och därmed bildningen av SOA. Resultaten visar att jämvikten i fasfördelning mellan gas- och partikelfas går att förutsäga under vissa omständigheter, exempelvis när luften i atmosfären inte är påverkad av människor. När luften däremot är påverkad av mänskliga utsläpp går det inte att på samma sätt förutsäga fasfördelningen eftersom partiklarnas upptagningsförmåga av organiska ämnen som är mycket oxiderade, d.v.s. de ämnen som i hög grad bidrar till bildning av partiklar i atmosfären ändrats och att aerosolerna inte är i jämvikt.

Nyckelord: Gas till partikelomvandling, flyktighet, sekundära organiska aerosoler, FIGAERO, CIMS, monoterpener, isopren, biogena ämnen, mänsklig påverkan, SOA.

List of publications

Publications included in this thesis work

- I. **Influence of Humidity, Temperature, and Radicals on the Formation and Thermal Properties of Secondary Organic Aerosol (SOA) from Ozonolysis of β -Pinene.**
Emanuelsson, E. U., Watne, Å. K., Lutz, A., Ljungström, E., & Hallquist, M. (2013). *The Journal of Physical Chemistry A*, 117(40), 10346-10358. doi:10.1021/jp4010218
- II. **High-Molecular Weight Dimer Esters Are Major Products in Aerosols from α -Pinene Ozonolysis and the Boreal Forest.**
Kristensen, K., Watne, Å. K., Hammes, J., Lutz, A., Petäjä, T., Hallquist, M., . . . Glasius, M. (2016). *Environmental Science & Technology Letters*, 3(8), 280-285. doi:10.1021/acs.estlett.6b00152
- III. **Gas to Particle Partitioning of Organic Acids in the Boreal Atmosphere**
Lutz, A., Hallquist, M., Mohr, C., Le Breton, M., Lopez-Hilfiker, F. D., and Thornton, J. A., Submitted to *Earth and Space Chemistry* (2019)
- IV. **Highly functionalized organic nitrates in the southeast United States: Contribution to secondary organic aerosol and reactive nitrogen budgets.**
Lee, B. H., Mohr, C., Lopez-Hilfiker, F. D., Lutz, A., Hallquist, M., . . . Thornton, J. A., (2016). *Proceedings of the National Academy of Sciences of the United States of America* 113 (6), 1516-1521. doi: 10.1073/pnas.1508108113
- V. **Gas and particle contributions of organic acids outside Beijing**
Lutz, A., Priestley, M., Salvador, C. M., Le Breton, M., Hallquist, Å. M., Pathak, R. K., Wang, Y., Zheng, J., Yang, Y., Guo, S., Hu, M., and Hallquist, M., Manuscript, (2019)

Publications not included in this thesis work

- i. A novel method for online analysis of gas and particle composition: description and evaluation of a Filter Inlet for Gases and AEROsols (FIGAERO).**
Lopez-Hilfiker, F. D., Mohr, C., Ehn, M., Rubach, F., Kleist, E., Wildt, J., Mentel, T. F., Lutz, A., Hallquist, M., Worsnop, D., and Thornton, J. A. (2014). *Atmospheric Measurement Techniques*, 7(4), 983-1001, doi: 10.5194/amt-7-983-2014
- ii. Molecular Composition and Volatility of Organic Aerosol in the Southeastern US: Implications for IEPDX Derived SOA.**
Lopez-Hilfiker, F. D., Mohr, C., D'Ambro, E. L., Lutz, A., Riedel, T. P., Gaston, C. J., Iyer, S., Zhang, Z., Gold, A., Surratt, J. D., Lee, B. H., Kurten, T., Hu, W. W., Jimenez, J., Hallquist, M., and Thornton, J. A. (2016). *Environmental Science & Technology*, 50(5), 2200-2209, doi: 10.1021/acs.est.5b04769
- iii. Ambient observations of dimers from terpene oxidation in the gas phase: Implications for new particle formation and growth.**
Mohr, C., Lopez-Hilfiker, F. D., Yli-Juuti, T., Heitto, A., Lutz, A., Hallquist, M., D'Ambro, E. L., Rissanen, M. P., Hao, L. Q., Schobesberger, S., Kulmala, M., Mauldin, R. L., Makkonen, U., Sipila, M., Petaja, T., and Thornton, J. A. (2017). *Geophysical Research Letters*, 44(6), 2958-2966.

Table of Contents

Abstract	iii
Sammanfattning	iv
List of publications	v
List of Abbreviations	viii
1. Setting the scene.....	1
2. Organic compounds in the atmosphere	3
2.1 Classification of particles in the atmosphere.....	3
2.2 Gaseous organic compounds in the atmosphere	4
2.3 Oxidation of organic compounds	5
2.4 Secondary organic aerosol formation.....	10
2.4.1 Saturation vapour pressure	11
2.4.2 Particle formation.....	15
3. Studying partitioning and volatility.....	17
3.1 G-FROST	17
3.2 Ambient measurements	18
3.3 VTDMA	19
3.4 FIGAERO-ToF-CIMS	21
4. Results and discussion.....	27
4.1 Oxidation of VOC in a controlled environment.....	27
4.2 Observations under ambient conditions	32
5. Atmospheric implications	43
Acknowledgements	47
References.....	49

List of Abbreviations

AMS – High Resolution Time of Flight Aerosol Mass Spectrometer
BSQ – Big Segmented Quadrupole
AVOC – Anthropogenic Volatile Organic Compounds
BVOC – Biogenic Volatile Organic Compounds
ToF-CIMS – Time of Flight Chemical Ionization Mass Spectrometer
CI* – Criegee Intermediate
CPC – Condensation Particle Counter
DMA – Differential Mobility Analyser
ELVOC – Extremely Low Volatile Organic Compounds
FIGAERO – Filter Inlet for Gases and Aerosols
G-FROST – Göteborg Flow Reactor for Oxidation Studies at Low Temperature
HOM – Highly Oxidized Multifunctional Organic Compounds
IMR – Ion Molecule Reaction
LVOC – Low Volatile Organic Compounds
MCP – Multi-Channel Plate
PM – Particulate Matter
RH – Relative Humidity
pON – Particle Organic Nitrates
 p_s – Saturation Vapor Pressure
SCI – Stabilised Criegee Intermediate
SMEAR II – Station for Measuring Forest Ecosystem Atmosphere Relations
SMPS – Scanning Mobility Particle Sizer
SOA – Secondary Organic Aerosols
SOAS – Southern Oxidant and Aerosol Study
SSQ – Small Segmented Quadrupole
ToF – Time of Flight
VFR – Volume Fraction Remaining
VOC – Volatile Organic Compounds
VTDMA – Volatility Tandem DMA

1. Setting the scene

Aerosols influence our life in various ways. The air we breathe is an aerosol and clouds in the sky are aerosols. Aerosols are formed when waves break and when a combustion engine is started. Complex chemical reactions in the atmosphere create aerosols. The particle phase of aerosols largely impact our climate by absorbing and scattering light (Stocker 2013). Aerosols adversely affect human health by increasing the risk of cardiovascular diseases, asthma attacks, cancer and premature death (Kim et al. 2015). Among the environmental health risks for humans, poor air quality is ranked as the highest (Shiraiwa et al. 2017).

An aerosol comprises solid or liquid particles suspended in a gas. To be defined as an aerosol, the particles have to be stable for some time. In the lower troposphere particles normally have a lifetime on the timescale of one day to a couple of weeks. However, if they reach the stratosphere they can stay for a long time, up to a year or more (Hinds 1998). Particles can originate from both natural and anthropogenic sources, and once they are in the air the sources can be difficult to distinguish from each other. Natural sources of particles include sea spray, dust and volatile organic compounds (VOC) emitted by vegetation. Combustion caused by humans, biomass burning and car exhaust fumes are examples of anthropogenic sources.

Secondary organic aerosols (SOA) is formed from oxidation of VOC in the atmosphere and they contribute significantly to the organic aerosol budget. VOCs can be biogenic or anthropogenic in their origin. The largest global contribution of VOCs comes from natural sources such as plants and trees (Hallquist et al. 2009). In many climate models, the sources of SOA are greatly simplified, if considered at all, resulting in considerable uncertainty about how SOA affect our climate (Tsigaridis et al. 2014). Therefore, it is important to determine how SOA is formed and how it is affected by anthropogenic pollution (Shrivastava et al. 2017).

More knowledge about SOA and its properties is needed to prevent further deterioration in human health, to make predictions about how our climate will change, and to take the appropriate remedial actions in these matters. The objective of this thesis is to contribute to the understanding of factors that play an important part in secondary particle formation, the chemical composition of secondary particles, and how the volatility of a compound influences its particle formation potential.

2. Organic compounds in the atmosphere

Oxidation of organic compounds is a fundamental process in atmospheric chemistry. It is estimated that only 10 000 to 100 000 organic compounds (Goldstein and Galbally 2007) of the potentially millions of organic compounds in an average 200 nm particle (Donahue et al. 2011) have been measured in the atmosphere. The atmosphere contains oxidizing species, creating new compounds via oxidation. Upon oxidation, some of the organic compounds will form products that are more prone to contribute to particle formation.

2.1 Classification of particles in the atmosphere

Atmospheric particles consist of several chemical compounds and these particles vary widely in size, from a few nanometers to almost 100µm, as illustrated in Figure 2.1.

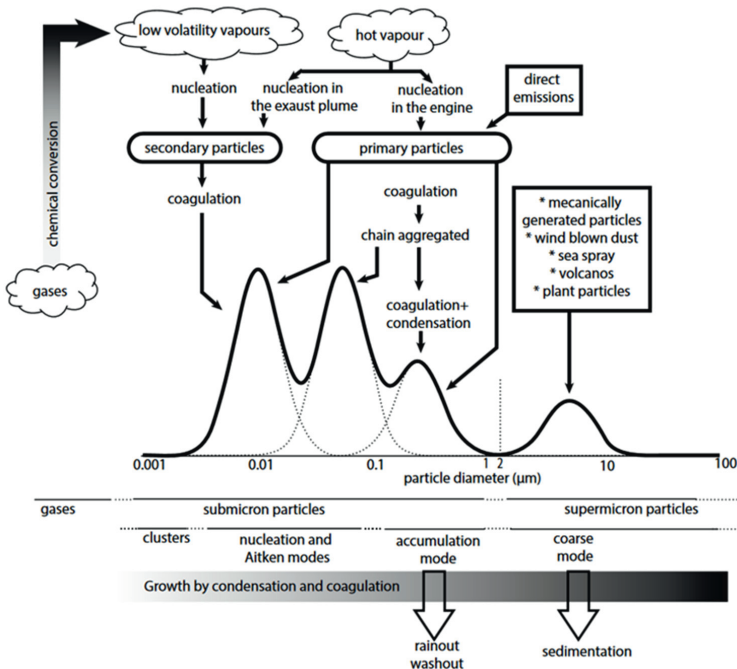


Figure 2.1 Classification of aerosol sizes, and sources and sinks of aerosols. Graphic design by Eva Emanuelsson. Printed with permission.

The smallest atmospheric particles, described by the nucleation and Aitken modes, are derived from high temperature combustion or atmospheric oxidation. They have a short lifetime, minutes to hours, and are removed by coagulation. Such small particles make a significant contribution to particle number, but little to particle mass (PM). The particles in the accumulation mode are still small enough to stay suspended in the air but also large enough not to coagulate, giving them a long lifetime of around 1-2 weeks. They are removed from the atmosphere via rainout or washout. Rainout is the process in which water condenses on a particle, forming a cloud, the particle eventually being removed by the next rainfall. Washout occurs when a particle is absorbed by a raindrop. Coarse mode particles, being 1 μm and larger, are primarily produced by mechanical processes. They are relatively heavy and their lifetime is short due to sedimentation. They make a significant contribution to PM, but little to particle number. Much of the legislation regarding particles is based on PM rather than particle number. Examples of this are $\text{PM}_{2.5}$ and PM_{10} , representing the mass of all particles smaller than 2.5 and 10 μm , respectively.

2.2 Gaseous organic compounds in the atmosphere

Volatile organic compounds (VOC) are gaseous organic compounds in the atmosphere. The greatest global contribution to VOC originates from plants, i.e. biogenic sources (BVOC). The amount of BVOC released from plants depends on sunlight intensity and leaf temperature (Guenther 1997). Plants may also emit BVOC when they are stressed by factors such as high temperatures or ozone levels (Niinemets 2010). These compounds protect the plants from outside attack (Loreto et al. 2014). BVOC also serve as a means of communication between plants and their pollinators (Loreto et al. 2014). It is estimated that 1000 Tg of BVOC are emitted to the atmosphere every year, the main constituent of which is isoprene, followed by methanol, ethanol, acetaldehyde, acetone, α -pinene, β -pinene, *t*- β -ocimene and limonene (Guenther et al. 2012). Atmospheric VOC from anthropogenic sources (AVOC), are emitted from many sources, such as combustion processes in the transport sector and by industry. In urban areas, AVOC may dominate over natural emissions (Borbon et al. 2013). Examples of common AVOC are aromatic hydrocarbons such as benzene, toluene, and *p*-xylene (Emanuelsson et al. 2013a).

2.3 Oxidation of organic compounds

Once VOC have been emitted into the atmosphere their usual fate is to become oxidized (Atkinson and Arey 2003). The relative importance of each oxidant depends on its concentration and the structure of its precursor. The most important oxidizing agents in the atmosphere are O₃, OH and NO₃. Oxidation by chlorine is mainly important in marine and some urban areas but will not be further discussed in this work.

2.3.1 Oxidants in the atmosphere

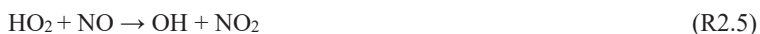
In rural areas the hydroxyl radical, OH, is primarily formed from photolysis of O₃, forming O(¹D), which in turn reacts with water via the following reactions (R2.1 and R2.2b).



The most common fate for excited oxygen, O(¹D), is to collide with another molecule, M, return to its ground state O(³P), see R2.2a, and consequently regenerate ozone through R2.7. In urban areas, however, OH is also formed from photolysis of gaseous nitrous oxide, HONO, and hydrogen peroxide, H₂O₂ (R2.3 and R2.4)



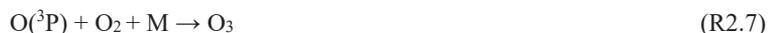
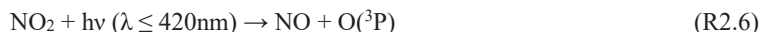
When the concentration of nitric oxide, NO, is high, as it is in polluted areas, it can react with the hydroperoxyl radical, HO₂ (R.2.5)



This reaction also converts other peroxy radicals into OH. OH being much more reactive thus R.2.5 catalyze reactions leading to smog formation in areas polluted by NO_x (George et al. 2015)

Reactions R2.1, R2.3 and R2.4 require sunlight, and OH is therefore often referred to as a daytime oxidant. OH is also formed during ozonolysis of alkenes, and this is the major OH production pathway at night.

Ozone is important for oxidation of unsaturated compounds during both day and night. The major formation pathway of tropospheric ozone is photolysis of NO₂, (see R2.6 and R2.7).



The primary source of NO_x is high temperature combustion, but it is also formed naturally in small quantities (e.g. from forest fires). Although the volume of NO_x from anthropogenic sources has decreased substantially in recent decades, due to the introduction of regulations and catalysts, some areas still suffer from high ozone levels due to the lack of control of NO_x emissions (Lefohn et al. 2010).

The nitrate radical, NO₃, is formed from the reaction of NO₂ with O₃, (R2.8).



However, during the day the NO₃ concentration is low since NO₃ is photo-dissociated.



For this reason, NO₃ is often considered a night time oxidant.

2.3.2 Oxidation of VOC

An important oxidation pathway for VOC is ozonolysis, which requires a double bond in the precursor VOC. The oxidation is initiated by the addition of O₃ to the double bond, resulting in the formation of a primary ozonide (POZ). It is unstable and may decompose in two ways, as shown in Figure 2.2, both pathways will form a carbonyl compound and a biradical, i.e. an excited Criegee Intermediate (CI*) (Finlaysson-Pitts 2000).

The branching ratio between the two scission pathways shown in Figure 2.2 depends on the structure of the R-groups, R being the abbreviation of any hydrocarbon structure. In the special case of a cyclic alkene the carbonyl group will be retained in the CI*. The CI* is in an excited state and can either be collisionally stabilized, forming a stabilized Criegee Intermediate (SCI), or decompose to an ester, acid, or hydroperoxide, alternatively the SCI dissociate to a carbonyl and a O(³P) (Finlaysson-Pitts 2000).

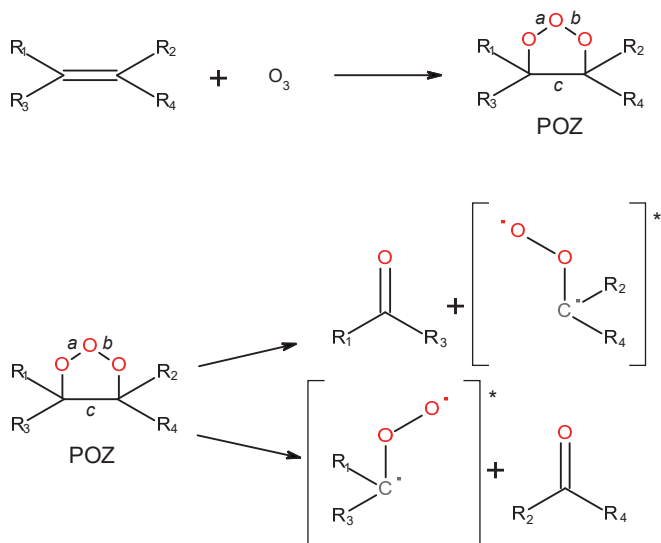


Figure 2.2 Schematic of the ozone reaction with a double bond, forming a primary ozonide (POZ) that decomposes either by scission of a and c or of b and c, forming a carbonyl compound and a Criegee Intermediate. R is the abbreviation of any hydrocarbon structure.

The most likely fate for many VOC during daytime is reaction with OH. The OH either abstracts one hydrogen from the VOC and forms water or is added to the double bond. Both cases yield an alkyl radical, R. The only reaction pathway important for R in the atmosphere is the addition of O₂, forming an alkylperoxy radical, RO₂. Figure 2.3 shows the possible reaction pathways for RO₂, with NO, HO₂ and self reaction with RO₂ being the most important pathways. Under low NO_x conditions, such as rural sites or chamber studies with no addition of NO_x, two reaction pathways compete: RO₂ can either react with itself, or with other RO₂ radicals, forming an alcohol, a carbonyl compound or an RO.

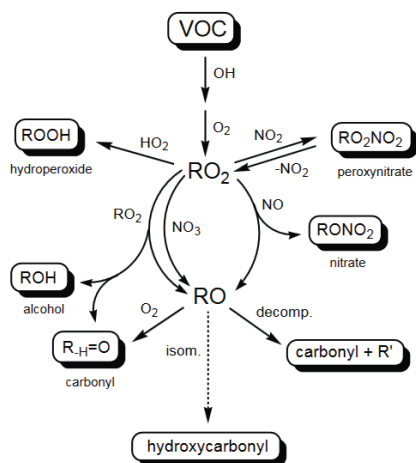


Figure 2.3 Schematic of OH-initiated VOC oxidation. Printed with permission (Hallquist et al. 2009).

levels, conversion from RO₂ to RO through the reaction with NO is the dominant pathway. The continued reaction of RO depends on the R-group, i.e. the parent compound. For larger R-groups the RO₂ can also react with NO to form organic nitrates, RONO₂. In addition, RO₂ can react with NO₂ forming peroxy nitrates, RO₂NO₂. Under high NO_x levels, the oxidation products of VOC are dominated by carbonyls, hydroxycarbonyls and organic nitrates, shown on the right in Figure 2.3 (Hallquist et al. 2009).

The other possibility is for RO₂ to react with HO₂, forming a hydroperoxide. The preferred reaction pathway depends on the structure of the R-group. The reaction proceeds via a tetroxide intermediate, R₁OOOOR₂, and the reaction rate is faster the more stable the intermediate, that is for larger R-groups. For small R-groups the HO₂ pathway is faster due to another reaction path being suggested, H-migration from HO₂ towards the RO₂ terminal oxygen (Vereecken and Francisco 2012). Under low NO_x conditions, products such as hydroperoxides, carbonyls, hydroxycarbonyls and alcohols are formed, shown on the left in Figure 2.3. At high NO_x

The Nitrate radical, NO₃, reacts with alkenes, primarily via addition to the double bond, as illustrated in Figure 2.4. The more substituted the alkene is, the faster the reaction rate (Finlaysson-Pitts 2000). This reaction leads to the formation of organic nitrates (ON), i.e. organic compounds containing a covalently bound –ONO₂ group. These nitrates affect air quality by acting as a reservoir of NO_x (NO and NO₂). Models estimate that isoprene reacting with NO₃ forming ON is responsible for removing 8% (Horowitz et al. 1998) to 30% (Liang et al. 1998) of anthropogenic NO_x from the boundary layer in the USA.

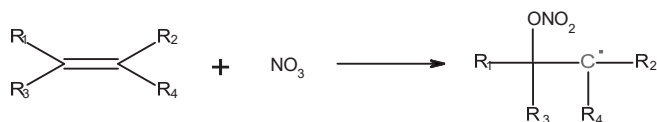


Figure 2.4 Nitrate radical reaction with an alkene forming an organic nitrate.

Like OH, NO₃ can also abstract a proton from the precursor to form nitric acid, (R2.10). This reaction is generally slow and not as important as the double bond reaction, although it contributes to the removal of NO_x from the atmosphere, by deposition of HNO₃ (Finlaysson-Pitts 2000).



In both NO₃ reactions, the formed radical (R) reacts with molecular oxygen (O₂) to form a peroxyradical, RO₂.

It was recently discovered that oxidation of monoterpenes leads to the formation of highly oxidized multifunctional organic compounds (HOM) (Ehn et al. 2012; Ehn et al. 2014; Jokinen et al. 2015). Very low volatile HOM are sometimes referred to as extremely low-volatility organic compounds (ELVOC). However, many HOM do not have sufficiently low volatility to be defined as ELVOC (Kurten et al. 2016). HOM are produced on the timescale of seconds from rapid auto-oxidation of RO₂ radicals. RO₂ radicals are produced in the initial oxidation steps of VOC. The mechanism is suggested to go through H-shifts, followed by O₂ addition (Ehn et al. 2014). The resulting RO₂ can then undergo a new H-shift followed by oxygen addition. In each step a hydroperoxide is formed, and an O₂ is added to the hydroperoxide, resulting in a peroxy radical group on the carbon where the hydrogen abstraction started (Ehn et al. 2014), as shown in Figure 2.5.

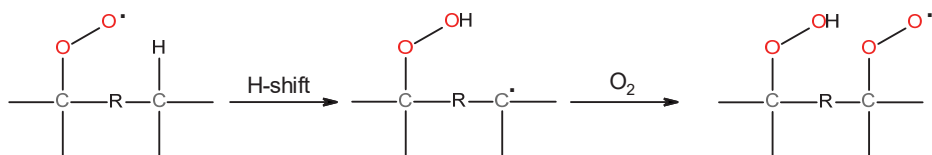


Figure 2.5 Hydrogen abstraction from RO₂ and concurrent O₂ addition. Mechanism suggested by Ehn et al. (2014). The newly formed RO₂ from the reaction can in turn undergo another H-shift followed by oxygen addition.

The fate of low volatility RO₂ is the same as for any RO₂ radical, i.e. reaction with HO₂, RO₂ or NO (Figure 2.3). The result of any of these reactions can be HOM and ELVOC formation, the precursor VOC and the relative abundance of oxidants determines how much of each species is formed (Ehn et al. 2014).

There is no strict definition of HOM, Trostl et al. (2016) define a HOM as C_xH_yO_z with $x = 8-10$, $y = 12-16$ and $z = 6-12$ for monomers, and dimers as C_xH_yO_z with $x = 17-20$, $y = 26-32$ and $z = 8-18$. The level of oxygenation of molecules in an organic aerosol is commonly used to describe the aerosol's characteristics and volatility. One measure of this is the molecules' oxygen to carbon ratio O/C; another popular method is to use the average oxidation state, *OS_C* (Kroll et al. 2011), defined to be

$$OS_C = 2 * O/C - H/C \quad (\text{Eq 2.1})$$

where *H/C* is the hydrogen to carbon ratio. The larger the value of *OS_C*, the more oxygenated the compound is. Compounds having an O/C ratio greater than or equal to 0.6 or an average oxidation state greater than or equal to 0 are often used as the lower limits for a HOM, see e.g. (Mutzel et al. 2015; Tu et al. 2016), although these measures should be used with care since CO₂ would also qualify as a HOM if they were used as definitions.

2.4 Secondary organic aerosol formation

A large fraction of atmospheric aerosols are of organic origin (Jimenez et al. 2009). Oxidation of BVOC leads to SOA formation, the oxidation agents can be natural or influenced by anthropogenic emissions (such as NO_x, R2.6 and R2.7). When a VOC is oxidized, many products will form, making atmospheric composition even more complex to model since each product will have different tendency to partition to the particle phase (Hallquist et al. 2009). SOA is estimated to contribute between 13–121 Tg/year (Tsigaridis et al. 2014) to the total organic aerosol budget. Primary organic aerosols (POA) are estimated to contribute between 34–144 Tg/year (Tsigaridis et al. 2014). However, models often underestimate the SOA burden compared with what is measured in the atmosphere (Volkamer et al. 2006). In order to improve these models, more knowledge about the formation and gas to particle partitioning of SOA is needed.

2.4.1 Saturation vapour pressure

The saturation vapour pressure, p_s , often referred to as the vapour pressure, is the pressure required to maintain mass equilibrium for one compound between gas and particle phase over a flat surface. When the partial pressure of a gas equals the p_s , no net mass will be transferred between the gas and solid/liquid phase. The lower the p_s of a compound, the larger the fraction will be found in the particle phase. In addition, the p_s is temperature-dependent, with lower temperatures yielding lower p_s . The saturation ratio, S_R , Eq 2.2, is defined as the partial pressure, p , of a compound divided by the p_s for the temperature of the system. A gas is saturated when its partial pressure is equal to the p_s (i.e., $S_R = 1$), and supersaturated when $S_R > 1$.

$$S_R = \frac{p}{p_s} \quad (\text{Eq 2.2})$$

The definition of p_s is for a flat surface. For nanometer sized particles, having a curved surface, the assumption that the surface is flat is not a good approximation. For those cases, the Kelvin effect has to be taken into account. The partial pressure, p_d , around the particle must be higher than p_s to maintain the diameter D_p and is defined to be

$$p_d(D_p) = p_s * \exp \frac{4\sigma M}{\rho R T D_p} \quad (\text{Eq 2.3})$$

where σ is the surface tension, M the molecular weight, ρ the density, R the common gas constant and T the temperature. The smaller the size of the particle, the higher the partial pressure over the particle has to be to maintain the particle diameter.

The p_s of a compound is a key property in describing how a compound partitions between gas and particle phase. It is one property that can be incorporated in models used to predict our future climate. For models to be accurate, a proper description of partitioning is necessary. Therefore considerable effort has been devoted to measuring the p_s of oxidation products from various VOC (Bilde et al. 2015; Bilde and Pandis 2001; Salo et al. 2010). Nevertheless, enormous discrepancies still exist between actual measurements of saturation vapour pressure and values predicted by these models (Donahue et al. 2011; Kurten et al. 2016).

If the structure of a molecule is known, the p_s can be derived using computational chemistry. Group contribution methods are a common way to accomplish this. They include calculations of the contribution of a structurally dependent parameter and the properties are established from the sum of the products of the frequency of each structural feature and its contribution. This method assumes that the effect of each molecular group is additive (Nannoolal et al. 2004). For example, a straight chain alkane acquires a lower p_s the more C-atoms are attached to it. At the same time, a branched alkane has a higher p_s than a straight one with the same number of C-atoms. In addition to this, functional groups in the molecule also affect the p_s . Several group contribution models for estimating p_s have been developed (Compernelle et al. 2011; Myrdal and Yalkowsky 1997; Nannoolal et al. 2008). However, these methods require that the structure of the organic aerosol constituent is known.

An organic aerosol is a complex mixture of various organic compounds, containing 5-10 million individual compounds in low concentration (Donahue et al. 2011). Currently knowledge of these compounds' identities is limited. Instruments that measure the molecular composition of the particles have been developed over the last decades. However, these methods do not reveal the chemical structure of the compounds, meaning the group contribution methods cannot be used. To overcome this problem Donahue et al. (2011) created a model that predicts the average p_s based on the numbers of C, O and H in the constituents. Donahue et al. (2011) use the term saturation mass concentration C^o ($\mu\text{g}/\text{m}^3$) instead of p_s in order to relate it to mass concentration, which is commonly used in atmospheric science. This makes it possible to estimate more easily and quickly the fraction of the compound in the particle phase, F_p .

$$F_{p,i} = \frac{[i]_{particle}}{[i]_{particle} + [i]_{gas}} \quad (\text{Eq 2.4})$$

$[i]_{particle}$ and $[i]_{gas}$ are the concentrations of compound i in the particle phase and gas phase. For example, consider the simplest possible case of an organic aerosol that consists of one compound, Y, and suppose the organic aerosol concentration is $1 \mu\text{g}/\text{m}^3$, the p_s of Y at 298K is $1.4 \cdot 10^{-5}$ Pa, and the molecular weight of Y is 180 g/mol. This does not tell us what fraction of Y is in the gas phase. If the p_s instead is expressed as saturation concentration, in this case of $1 \mu\text{g}/\text{m}^3$ for compound Y it is easy to calculate the fraction of material in the particle phase. In this case approximately 50% of the material is in the particle phase with an organic aerosol

concentration of $1 \mu\text{g}/\text{m}^3$. If however the organic aerosol concentration were to increase to $2 \mu\text{g}/\text{m}^3$, then approximately 66% of Y would be in the particle phase.

As was discussed earlier, the structure of a compound is important in describing its p_s , or saturation concentration. In work described in this thesis, a mass spectrometer that provides the exact mass, and thus the constituents' atoms, and not the structure of the molecules, has been used. In order to predict the simplified average saturation concentration, based on the atoms in a molecule, one first needs detailed information of known saturation concentrations.

Under VOC oxidation some compound classes are more likely to form than others. Figure 2.6 displays seven organic compound classes, important for SOA formation. Figure 2.7 displays experimentally obtained logarithmic saturation concentrations, plotted versus the number of

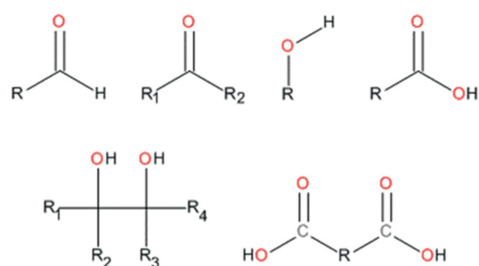


Figure 2.6 From the top left structures of: aldehyde, ketone, alcohol, carboxylic acid, diol and dicarboxylic acid.

carbons for the compound classes mentioned in Figure 2.6. Each class has a different functionality and varies only in the length of its carbon chain. Each carbon decreases the logarithmic saturation concentration by 0.475 (Donahue et al. 2011), indicated by the solid parallel lines for each class. The functionalization is shown by deviation from the hydrocarbon line. The oxygen functionality is not as straightforward: how the oxygen is bound

to the carbon affects the change in saturation concentration. An oxygen which is double bonded to a carbon, i.e. carbonyls, decreases $\log_{10}C^0$ by 1, while alcohol decreases $\log_{10}C^0$ even more, by about 2.3 (Donahue et al. 2011). It is impossible to determine how oxygen is bound using mass spectrometer data. To overcome this issue, Donahue et al. (2011) use an estimation method based on proxies for the distribution of functional groups and the use of only elemental composition as input.

Nitrate radical oxidation also forms compounds of lower saturation concentration. The addition of a nitrate group ($-\text{ONO}_2$) lowers the saturation concentration even more than oxygen does, approximately by 2.5 orders of magnitude (Donahue et al. 2011).

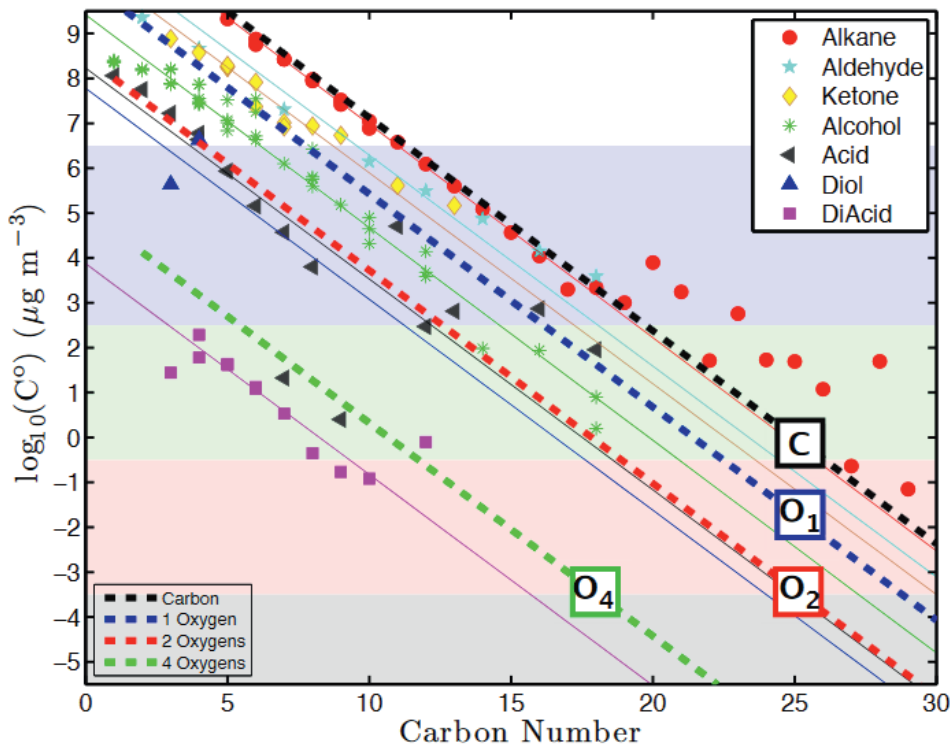


Figure 2.7 Logarithmic saturation concentration ($\log_{10}C^\circ$ ($\mu\text{g m}^{-3}$)) plotted against carbon number for seven organic compound classes. Each class has the functionality indicated by its color and varies only in the number of carbons it has. The slope of each line represents the effect of increasing the number of C-atoms, while deviation from the hydrocarbon line shows the functionalization. The dashed lines indicate the average decrease in $\log_{10}C^\circ$, 1.7 per O atom. Printed with permission (Donahue et al. 2011).

C° can thus be estimated based on molecular information that does not require information about the explicit molecular structure. In the work described in this thesis, an updated version of the Donahue et al. (2011) method was implemented, based on saturation concentrations for HOM, detected by Trostl et al. (2016), and calculated as

$$\log_{10}C_i^\circ = (n_o - n_c)b_c - (n_o - 3n_N)b_o - \left(\frac{(n_o - 3n_N)n_c}{(n_c + n_o - 3n_N)}\right)b_{CO} - n_N b_N \quad (\text{Eq 2.5})$$

where $n_0 = 25$, corresponding to the number of carbon atoms in a straight alkene having the saturation concentration of $1\mu\text{g}/\text{m}^3$; b_c is the carbon-carbon interaction term, set to $= 0.475$, which is the value each carbon atom lowers $\log_{10}C_i^\circ$; b_o is the oxygen-oxygen interaction

term, set to 2.0, representing how much each oxygen lowers the $\log_{10}C_i^o$; and b_{CO} is the carbon-oxygen non-ideality, which is set to -0.9, correcting for the non-linearity in Figure 2.7. The nitrogen-nitrogen interaction term $b_N = 2.5$, n_C , n_O and n_N are the numbers of carbons, oxygen and nitrogen atoms in the compound, respectively (Donahue et al. 2011). The update to the model is necessary since HOM have a slightly higher saturation concentration than previously predicted (Trostl et al. 2016). The reason for the under-prediction is the structure of HOM, which form via auto oxidation, is now known to incorporate a $-OOH$ functional group, lowering the saturation concentration less than the functional groups that had been assumed previously ($-OH$ and $=O$).

2.4.2 Particle formation

For a particle to form, a nucleus onto which the vapor condenses must exist. The nucleus can be formed either by homogeneous nucleation or by heterogeneous nucleation. In all gases, molecular clusters will form due to attractive forces between the molecules. The clusters are unstable and will disintegrate, but when a supersaturated vapor is formed more frequent collisions between clusters will occur. This will in turn lead to the formation of agglomerates. Some of these agglomerates will exceed a critical size, called the Kelvin diameter, d^* , creating a nucleus large enough to be stable, see Eq 2.3. When a supersaturated gas condenses on a nucleus of this type, it is called homogeneous nucleation. This type of nucleation occurs in the atmosphere for compounds with very low p_s . In the laboratory, however, homogenous nucleation can occur for compounds of higher p_s by creating a supersaturated vapour from high concentrations of the compound.

Heterogeneous nucleation, or nucleated condensation, is the process of particle formation when there is a pre-existing nucleus onto which the gas condenses. This is the process that makes it possible for compounds of higher p_s to form particles since much lower saturation ratios are needed for this kind of condensation.

2.4.3 Partitioning

Partitioning, in this context, is the physical process that describes how a species is distributed between the gas phase and the particle phase. To allow modelling of partitioning between gas

and particle phase, the model suggested by (Pankow 1994) that builds upon Raoult's law is used. The partitioning coefficient K_i is computed using the following formula

$$K_i = \frac{[i]_{particle}}{[i]_{gas} * M_{org}} = \frac{RT}{\overline{MW}_{om} \gamma_i * p_i^0} \quad (\text{Eq 2.6})$$

where M_{org} is the aerosol organic mass concentration, in this work measured by a High Resolution Time of Flight Aerosol Mass Spectrometer (hereafter referred to as AMS); $[i]_{particle}$ and $[i]_{gas}$ are the concentrations of compound i in the particle phase and gas phase, respectively; p_i^0 is the p_s of i ; γ_i is the activity coefficient; \overline{MW}_{om} is the mean molecular mass of the particle constituents; R is the gas constant; and T is the temperature. The activity coefficient, γ_i , accounts for deviations from ideal behavior for a compound in a mixture of chemical substances.

Another way to express the partitioning between gas and particle phase is in terms of saturation concentration, C^* , which is the inverse of K_i . The difference between C^0 and C^* is that C^0 is the saturation concentration over a pure liquid whereas C^* takes the activity coefficient into account, thereby allowing for the non-ideality present in the particle matrix. C^* is equivalent to $1/K_i$, thus C^* can be calculated in terms of Eq 2.6. Alternatively, the gas/particle ratio can be expressed in terms of Eq. 2.4.

$$C^0 * \gamma = C^* = M_{org} * \left(\frac{1}{F_{p,i}} - 1 \right) = M_{org} * \frac{[i]_{gas}}{[i]_{particle}} \quad (\text{Eq 2.7})$$

Thus the saturation concentration of a compound can be calculated if the concentration of the organic mass, the concentration of the compound in particle phase and the concentration of the gas phase are known.

3. Studying partitioning and volatility

In order to study aerosol formation and partitioning between the gas and particle phase, studies in both the lab and the ambient atmosphere are needed. Laboratory studies allow several parameters to be controlled and detailed knowledge and understanding obtained. The results of such studies can be incorporated in models used to predict our climate or air quality. To test such models, real-world measurements taken in the atmosphere are crucial.

3.1 G-FROST

The Göteborg Flow Reactor for Oxidation Studies at low Temperature (G-FROST) was used in papers I and II to study oxidation of VOC. G-FROST is a vertical laminar flow reactor in the form of a 191 cm glass tube with an inner diameter of 10 cm, located in a temperature-controlled chamber, as illustrated in Figure 3.1. The setup has been explained in detail elsewhere (Jonsson et al. 2006). In short, VOCs and an oxidant, e.g. ozone, are introduced through separate ports to the reactor. The oxidant and the VOC are mixed in an injector and particles are formed in the tube as the reactants are oxidized. Compounds of lower volatility will form as the oxidant and VOC travel through the tube. The gases are continuously led through the reactor at a constant rate, thus the age of the aerosol at the sampling location is always the same. Measurement instruments are connected to the sampling ports at the end of the tube. When using G-FROST, compounds are oxidized under controlled conditions, which provides an advantage over many other so-called static reactors, where the conditions change during the experiment. Relative humidity (RH), pressure and temperature are controlled during the experiments and the gas flow is set by mass flow controllers. Since the aerosol age can be kept stable at the point of measurement, instruments with low time resolution can be used.

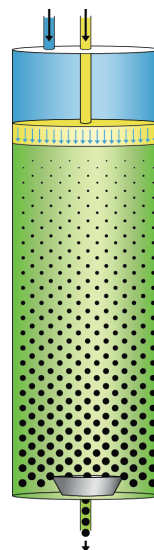


Figure 3.1 The principle of G-FROST. The oxidant and reactant are delivered to the reactor with a constant flow. They are mixed in an injector (shown in yellow) and particles form in the tube. At the sampling port, aerosol of the same age is formed. Design by Eva Emanuelsson. Printed with permission.

When monoterpenes are oxidized by ozone, OH-radicals are formed. An OH-scavenger reacts with OH-radicals, making it possible to solely study oxidation by ozone without influence of OH. In G-FROST an OH-scavenger can be introduced into the system. An additional effect of using an OH-scavenger is that the HO₂/RO₂ ratio is altered. This leads to different product distributions, and provides important information regarding the chemistry of the radicals. When 2-butanol is used, more HO₂ will form leading to a higher HO₂/RO₂ ratio. The addition of cyclohexane as an OH scavenger decreases the HO₂ concentration, thus decreasing the HO₂/RO₂.

3.2 Ambient measurements

This thesis will present results from field measurements from three different locations (papers III - V): a rural site in Hyytiälä, Finland, a rural site affected by anthropogenic emissions in Centreville, Alabama, USA, and a semi-urban site in Beijing, China.

The Station for Measuring Forest Ecosystem Atmosphere Relations (SMEAR II), is situated in Hyytiälä, Finland, 220 km north-west from Helsinki. The measurement station has been described in detail previously (Hari and Kulmala 2005). The station is situated in a boreal forest that consists of Scots Pine, which is representative of the boreal coniferous forests that cover 8% of the Earth's surface. The nearest city, Tampere, having 200 000 inhabitants, is located 60 km south-west from the site, making the site a remote measurement station (Hari and Kulmala 2005). The measurements were performed during spring (April-May 2013), the time of year when the concentration of α -pinene dominates the VOC budget (Hari and Kulmala 2005).

The measurement campaign Southern Oxidant and Aerosol Study (SOAS) was deployed near Centreville, USA, in June-July 2013; a detailed description of the campaign has been provided by Xu et al. (2015) and Carlton et al. (2018). The location is 50 km south-east of Tuscaloosa, having 95 000 inhabitants, and 80 km southwest of Birmingham, having a population of 210 000. The station was situated in a temperate forest consisting of mixed deciduous trees (oak-hickory) and loblolly pine (Hansen et al. 2003). The dominating VOC emitted is isoprene, but monoterpenes also make some contribution. In addition, the site is influenced by anthropogenic pollution, such as NO_x and SO₂ (Fisher et al. 2016). The temperature has increased in most locations in the world due to global warming (Stocker

2013). However, the southeast United States has not warmed during the last century, despite high rates of anthropogenic pollution. The reason for this is not clear, but it has been suggested that sulfur dioxide emissions react with naturally occurring VOC to form SOA (Carlton et al. 2018). The SOA in turn reflects the incoming light, resulting in no net heating. Therefore, the southeast United States is an ideal place to investigate fundamental atmospheric processes, such as how biogenic emissions and anthropogenic pollution interact, and how they affect atmospheric chemistry and consequently air quality and climate. This knowledge is crucial to learning how the effects of climate change might be mitigated or reduced (Carlton et al. 2018).

In Beijing, measurements were performed 40km north-east of Beijing close to Changping town in May and June 2016 (Le Breton et al. 2018). The measurement campaign was conducted with a focus on pollution episodes in north-eastern China. Pollution episodes, defined as periods of high PM_{10} concentration, were observed with a maximum PM_{10} concentration reaching $115 \mu g/m^3$. During the episodes, concentrations of organic, sulfate and nitrate aerosols were high, although the fractions were not correlated (Le Breton et al. 2018).

3.3 VTDMA

A Volatility Tandem Differential Mobility Analyzer (VTDMA) measures the difference in particle diameter before and after heating. This gives a measure of the aerosol volatility and has been described in detail by Jonsson et al. (2007). The VTDMA consists of two Differential Mobility Analyzers (DMAs) with several ovens in between. After the second DMA there is a Condensational Particle Counter (CPC), as shown in Figure 3.2. In the first DMA one size of the poly-disperse particles from the aerosol is selected. The resulting monodisperse particles are then heated stepwise from $25^\circ C$ to $330^\circ C$ in the eight oven units, each oven having a different temperature range. After heating, the particles' diameters are measured in the second DMA and their number concentration is measured by the CPC. Before the aerosol enters the first DMA, a Nafion® dryer can be connected to dry the aerosol. This ensures that the difference in particle diameter is due to evaporation of organic compounds and not of water from the particles' surface.

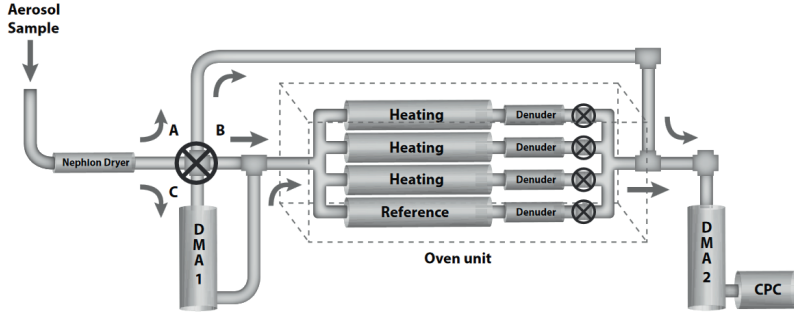


Figure 3.2 The VTDMA. In DMA 1, one size of the poly-disperse particles is selected. The monodisperse particles are heated in a selected oven unit. The resulting diameter is measured in DMA 2 and the number concentration measured by the CPC. Before the aerosol enters the first DMA, a Nafion® dryer dries the aerosol. Design by Eva Emanuelsson. Printed with permission.

Volume Fraction Remaining at an evaporation temperature T , VFR_T , is derived from the mode of the particles' diameter (D_p) at an evaporation temperature, T , to evaluate the volatility of the particles. The diameter is normalized to the reference diameter (D_{pRef}) selected by the first DMA and cubed.

$$VFR_T = \left(\frac{D_p}{D_{pRef}} \right)^3 \quad (\text{Eq 3.1})$$

In order to obtain the full evaporation profile, the result of several such measurements can be plotted versus the evaporation temperature, generating a thermogram, as illustrated in Figure 3.3.

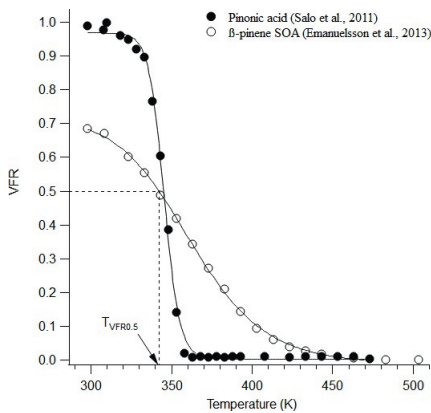


Figure 3.3 Thermograms from pure pinonic acid and β -pinene SOA.

3.3. There the VFR for the pure component pinonic acid is compared with that of β -pinene SOA. β -pinene clearly has a different desorption profile to pinonic acid, although the temperature where 50% of the particles' volume has evaporated, $T_{VFR0.5}$, is roughly the same, underlining the importance of including the steepness of the function. The shape of each thermogram is best fit by a sigmoidal function of the form given in Eq 3.2. The sigmoidal fits provide consistency and the ability to compare thermograms.

$$VFR_T = VFR_{\min} + \frac{(VFR_{\max} - VFR_{\min})}{1 + \left(\frac{T_{\text{position}}}{T}\right)^{S_{VFR}}} \quad (\text{Eq 3.2})$$

The expression includes both the steepness, S_{VFR} , of the thermogram and its mid-position, T_{position} . The free parameters VFR_{\max} and VFR_{\min} define the boundaries of the highest and lowest VFRs, respectively. In order to more strictly define the most volatile and the non-volatile fraction, the equation can be used to derive specific VFRs at 298K and 523K, (VFR_{298} and VFR_{523}). In addition, $T_{VFR0.5}$, the temperature where half of the particles' volume is evaporated, can be calculated. $T_{VFR0.5}$ is a general measure of the volatility, whereas S_{VFR} is a measure of the distribution of the volatilities of the major components of the particles.

3.4 FIGAERO-ToF-CIMS

Mass spectrometry is a method to separate ions in the gas phase, based on their mass to charge ratio (m/z), and requires the molecules of interest to be ionized. The chemical ionization high-resolution time-of-flight mass spectrometer (ToF-CIMS, Aerodyne Research, Inc., USA) ionizes target molecules by soft ionization and enables measurement of the gas phase composition. Soft chemical ionization minimizes fragmentation and facilitates identification of the parent molecule in ionic form, as opposed to hard ionization where the parent molecule is ionized through fragmentation. The mass spectrometer has a high resolution with a mass resolving power of >5000 ($M/\Delta M$). The mass resolving power, R , describes the separation of two mass peaks, given by

$$R = \frac{M}{\Delta M} \quad (\text{Eq 3.3})$$

where M is the mass of the singly charged ion in the mass spectrum and ΔM is the width of the peak at full width half maximum. The higher the value of R , the better the two peaks in the spectrum (and thus the ions) can be separated. High resolution power is a prerequisite for performing high resolution peak fitting, meaning that two or more compounds of the same nominal mass can be separated.

Chemical ionization may be performed with various compounds as reagent ions, depending on the nature of the target molecule. Chemical ionization performed in this work used acetate

and iodide as reagents. Furthermore, two different ionization mechanisms – a radioactive alpha particle emitter and an X-ray source – were used to ionize the reagent ion. In Hyttiälä 2013 and SOAS 2013 (papers III and IV) acetate was used as the reagent ion, with polonium (^{210}Po) as the ionizer, resulting in the generation of negative ions. Thus, the mass spectrometer operated in negative ion mode. The acetate ion, CH_3COO^- , is produced by passing acetic anhydride, $(\text{CH}_3\text{CO})_2\text{O}$ with dry, pure, nitrogen through a (^{210}Po), radioactive alpha source. The resulting CH_3COO^- ion abstracts a proton from the target molecule, producing negative ions. The acetate ion has low gas phase acidity and so does not abstract protons from VOCs with high pKa such as alcohols, ketones, and aldehydes. It does extract protons from carboxylic acids, making it an ideal selective reagent ion for carboxylic acid detection (Veres et al. 2008). In China (paper V) methyl iodide was used as the reagent ion, and a Tofwerk X-ray source (type P, operated at 9.5 kV and 150 μA) was used to produce I^- , the reagent ion, which is good at forming adducts (Lee et al. 2014). In both ionization schemes, the chemical ionization takes place in the Ion Molecular Reaction (IMR) chamber, shown in Figure 3.4, kept at approximately 100 mbar for acetate, and 500 mbar for iodide. After being ionized, the target molecules are guided and focused by two quadrupoles, the small segmented quadrupole (SSQ) where the collisional dissociation occurs, and then focused by the big segmented quadrupole (BSQ). The ion optics focuses and accelerates the ion before it enters the Time of Flight (ToF) using high frequency pulses. In the ToF region, the ions travelling time, i.e. the “time of flight”, is measured before they are detected on a multi-channel plate (MCP). The MCP measures the molecular mass to charge ratio (m/z) of the ions with high accuracy. The intensity of the signal is proportional to the concentration of the compounds.

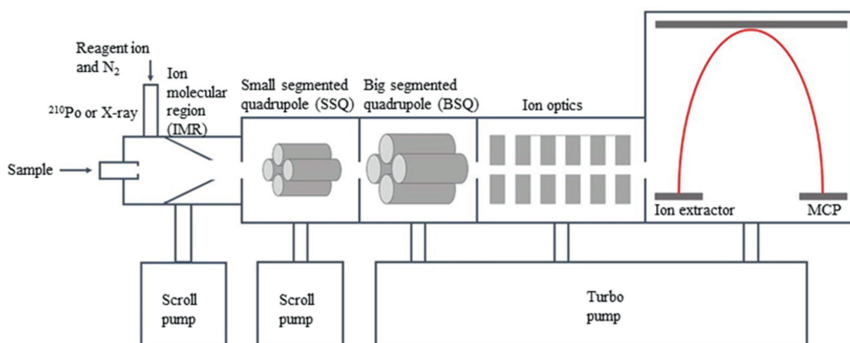


Figure 3.4 Schematics of the high-resolution time-of-flight chemical ionization mass spectrometer (ToF-CIMS). Graphic design by (Sanchez et al. 2016). Printed with permission.

The data from ToF-CIMS was analyzed with tofTools, a MATLAB toolbox (<http://www.junninen.net/tofTools>) an open source project developed by the department of physics at University of Helsinki. The raw data in the ToF-CIMS was recorded every second. In order to save computational time and increase the signal-to-noise-ratio, the data was averaged over a 30-second period before analysis. Mass calibration was performed on each averaged spectrum. The mass spectrometer has to be calibrated to specify which peak corresponds to which mass. For mass calibration, several species can be used, but only the mass calibrants with the best signals are used in each calibration. This means that different masses may be used when calibrating different spectra. This feature is very useful when any of the calibrants have a poor signal in a subset of the data. An average peak shape is calculated. The peak shape is based on all peak shapes of the spectra and the ones having the greatest resolution are used to calculate an average peak shape for each mass. The averaged peak shape is used to assign one or more compounds to each unit resolution peak in the spectra.

The ToF-CIMS is limited to measurements of compounds in the gas phase. To retrieve information about the compounds in the particle phase, a new inlet named the Filter Inlet for Gases and Aerosols (FIGAERO), was developed (Lopez-Hilfiker et al. 2014). It is connected to the ToF-CIMS, henceforth referred to as FIGAERO-ToF-CIMS. The FIGAERO inlet, Figure 3.5, allows for quasi-simultaneous measurements of compounds in particle and gas phase. It operates in two modes: 1) sampling of the gas phase and simultaneous collection of particles on a filter, and 2) desorption of particles from the filter with temperature-controlled, heated, high-purity nitrogen gas, where the volatilized particles are directly introduced into the ionization region and measured in the gas phase (Lopez-Hilfiker et al. 2014).

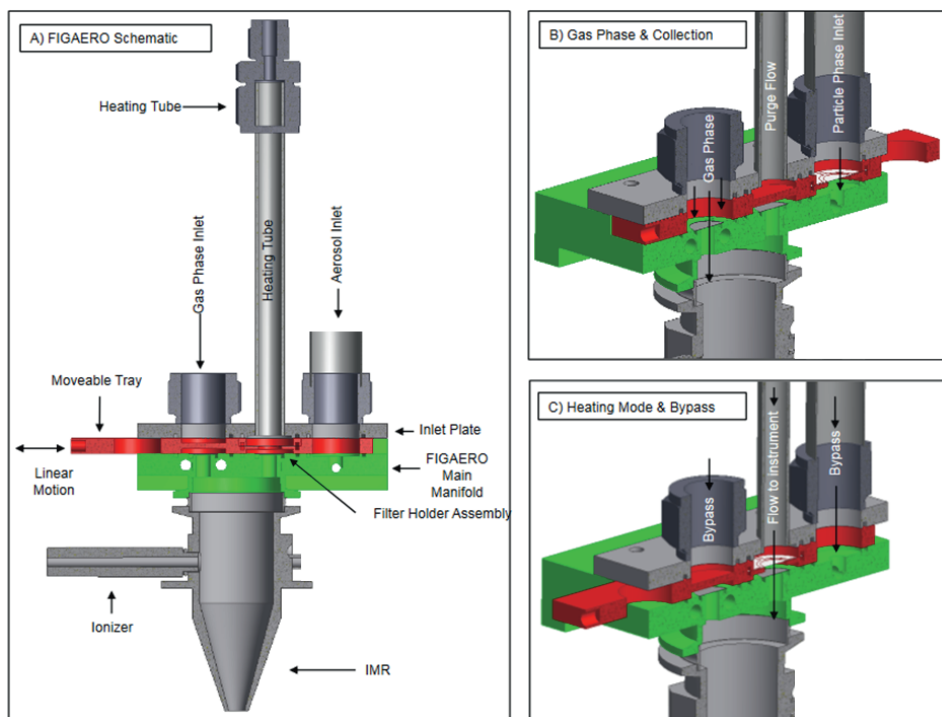


Figure 3.5 Schematic of the FIGAERO. A) Overview. The main manifold (green) and the movable tray (red) are made from Teflon. The manifold connects the FIGAERO with the CI-HR-ToF-MS. The movable tray switches between collection mode and desorption of particles. B) Gas measurement and particle collection mode. In this mode, the desorption port is blocked by the tray. C) Desorption mode. The tray has moved the filter to the position under the heating tube, and heated N_2 passes over the filter. The N_2 gas is heated to desorb the components on the filter. The resulting vapors are analyzed in the mass spectrometer. Graphic design by Lopez-Hilfiker et al. 2014. Printed with permission.

In order to analyze particle composition, the particles are desorbed thermally by increasing the temperature of the N_2 from ambient ($\sim 25^\circ\text{C}$) to 200°C in Hyytiälä and at SOAS (paper III and IV) and to 250°C in China (paper V). The temperature was maintained at the highest temperature for several minutes in order to ensure that all material was desorbed. The particle phase data were then analyzed with tofTools, with some additional analysis. A desorption profile (thermogram) is obtained, as the particles evaporate from the filter, detected in the gas phase, as shown in Figure 3.6 This type of thermogram differs from the one obtained using VTDMA. In the FIGAERO thermogram, the signal for each ion is plotted against temperature, rather than the VFR. The temperature at which most of a given compound evaporates, i.e. when the number of ion counts is at a maximum, is referred to as the compound's T_{max} . The thermograms were analyzed in detail in paper III.

It has been observed that it is common for a desorption profile to be bimodal (Lopez-Hilfiker et al. 2015), as can be seen in Figure 3.6. This has been attributed to either the presence of isomers having different p_s or, more likely, thermally decomposed compounds of higher molecular weight, since the peaks are relatively well separated (Lopez-Hilfiker et al. 2015). In order to address this, all desorptions are analyzed with a custom nonlinear least-squares peak-fitting routine that finds the maximum of all peaks. First, desorptions with one maximum (i.e. T_{\max}) were fitted to obtain a representative desorption peak shape. The remaining desorptions were then fitted using this peak shape. The numbers of peaks per desorption were allowed to vary from one to a maximum of three, in order to reduce over-fitting. The thermogram was fitted with software originally developed by the Department of Atmospheric Sciences, University of Washington and then further developed as part of this work. The program is based on an iterative algorithm (Levenberg–Marquardt) using nonlinear least squares to find the best fit. For a pure compound, the desorption peak shape can vary by up to 30% (Lopez-Hilfiker et al. 2015), therefore the standardized peak shape was allowed to vary by the same percentage. In order to receive the signal of each compounds' contribution to the thermogram, each peak in a multimodal thermogram was integrated separately.

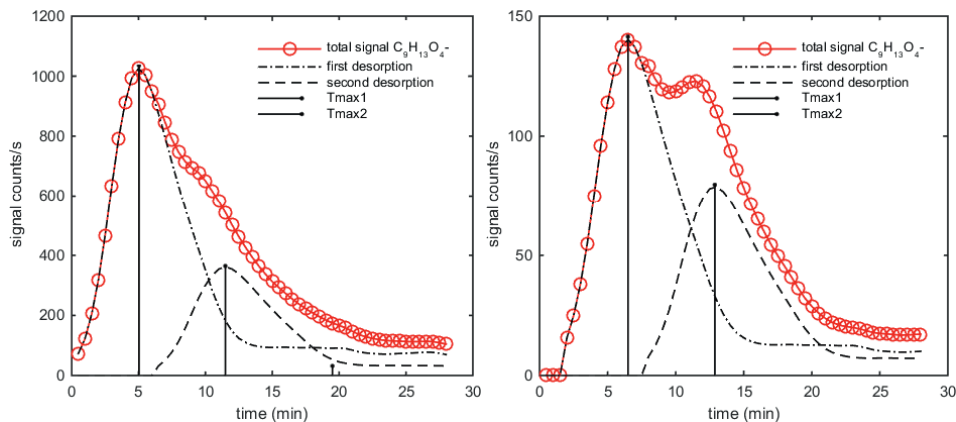


Figure 3.6 Two desorption profiles from the $C_9H_{13}O_4^-$ fragment taken at different times. Two T_{\max} are obtained for all thermograms of this ion. The temperature at which most of a particular compound evaporates, i.e. when the number of ion counts is at a maximum, is derived from the temperature at that specific time, and is referred to as T_{\max} . For fitting purposes the thermograms are fitted versus time instead of temperature, since the highest temperature are held constant for several minutes. The time is then converted to temperature. The heating regime differs slightly in each case, hence the difference in time for the obtained maximum signals (this does not affect the T_{\max}).

4. Results and discussion

The objective of this thesis is to contribute to the understanding of factors that are important for secondary organic particle formation, the chemical composition of these organic particles, and how a compound's volatility affects the compound's potential for particle formation. Papers I and II focus on controlled lab studies of β -pinene and α -pinene, which were undertaken to gain a better understanding of the fundamentals of oxidation of VOC. In addition, field studies were conducted in three different locations: a remote boreal forest in Europe, a semi remote forest in the USA, and one urban area in Asia. The results of these studies are presented in papers III, IV and V

4.1 Oxidation of VOC in a controlled environment

In paper I, the effect of relative humidity, temperature and radical chemistry on ozonolysis of β -pinene was investigated using the G-FROST facility. Figure 4.1 shows the major β -pinene ozonolysis pathways. As can be seen in R3a, water is important for the formation of the highly volatile compound nopinone. Upon β -pinene ozonolysis, both particle number and mass concentration decrease as humidity increases. In earlier studies with the monoterpenes, limonene, α -pinene and Δ^3 -carene, particle mass was seen to increase with increased humidity (Jonsson et al. 2006; Jonsson et al. 2008; Jonsson et al. 2007). In these earlier studies, the effect of relative humidity on number concentration also depended on other parameters such as temperature and whether a scavenger was used or not.

The difference between β -pinene and the other monoterpenes can be explained by the structures of the molecules. β -pinene differs from limonene, α -pinene and Δ^3 -carene by having an exocyclic double bond, i.e. the double bond is outside the ring. α -pinene and Δ^3 -carene have endocyclic double bonds, and limonene has both an endo- and an exocyclic double bond. In limonene, the ozone reacts preferentially with the endocyclic double bond (Maksymiuk et al. 2009; Pathak et al. 2012).

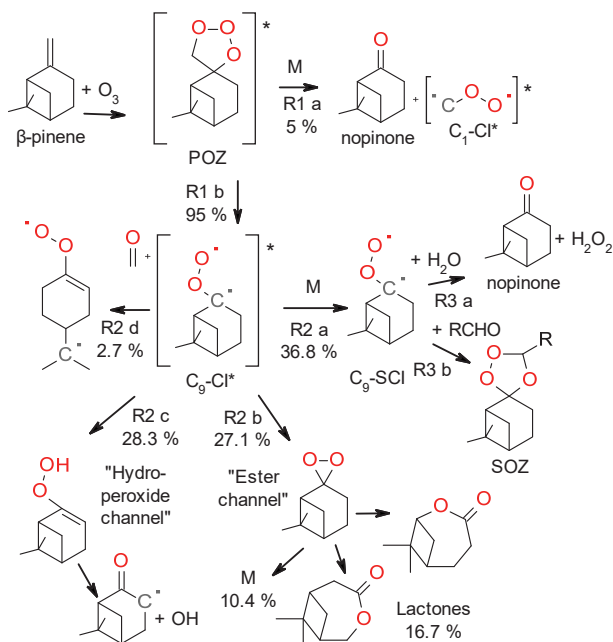


Figure 4.1 Schematic of the major pathways in β -pinene ozonolysis. The routes and yields are from (Nguyen et al. 2009), omitting pathways with yields below 1%. Reactions 3a and 3b are suggested by (Winterhalter et al. 2000).

When ozone is attached to the exocyclic bond in β -pinene, forming a primary ozonide (POZ) the ring structure remains intact, shown in Figure 4.1 (R1a and R1b). This results in compounds with high p_s , relative to compounds in which the ring structure is broken. When ozone attaches to an endocyclic double bond, ring opening will occur and all carbons will be retained in the molecule, leading to oxygenated compounds with lower p_s , as illustrated in Figure 4.2.

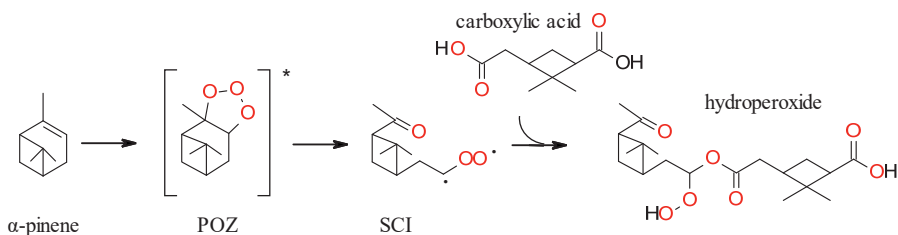


Figure 4.2 Simplified representation of proposed reaction responsible for the formation of hydroperoxide from paper II. The stabilized Crigee Intermediate, formed from α -pinene ozonolysis, reacts with a carboxylic acid, in this case pinic acid.

There are two possible pathways for the POZ from β -pinene: the dominant pathway is formation of a C₉-CI* and formaldehyde; the volatile compound nopinone and a C₁-CI* will also form, but to a much lower extent (5%) (Nguyen et al. 2009). The C₉-CI* is in an excited state and has four possible pathways: collisional stabilization, ester channel, hydroperoxide channel or opening of the inner ring.

Previous work has established that SOA particle formation increases with increased humidity (Docherty et al. 2005; Jonsson et al. 2008; Keywood et al. 2004). The differences in the effect of humidity for α -pinene and β -pinene were attributed to the difference in position of the double bond, arguing that an exocyclic double bond would increase the HO₂/RO₂ ratio, leading to more highly volatile compounds and thus less SOA (Docherty et al. 2005; Keywood et al. 2004). In paper I, decreased SOA production was observed as the HO₂/RO₂ ratio increased. Here cyclohexane and 2-butanol were used as OH-scavengers, the particle mass and number concentration decreased in the following order: no scavenger >> cyclohexane > 2-butanol. However, a high relative humidity would also lead to a decrease in the HO₂/RO₂ ratio, via the water dependence on the HO₂ self-reaction. This provides an inconsistency in attributing our observations of the ozonolysis of β -pinene to a direct water effect on HO₂/RO₂, as previously suggested by Docherty et al. (2005) and Keywood et al. (2004). The volatility of the particles in paper I were monitored by keeping the evaporative temperature in the VTDMA oven at 383K and then calculating the VFR as the parameter VFR₃₈₃. In all experiments, VFR₃₈₃ decreased with increased humidity, meaning an increase in volatility. This effect was especially pronounced in the low temperature cases. Generally, more volatile particles were produced when 2-butanol was used as OH-scavenger than when cyclohexane was used. Cyclohexane gave more volatile particles than the no scavenger experiments and this was manifested by a decrease in VFR₃₈₃.

The thermal properties of particles in paper I were also affected by changes in relative humidity and radical chemistry for β -pinene. As expected from Raoult's law, the lower temperature experiments favoured nucleation. Furthermore VFR₃₈₃ decreased with increasing temperature in G-FROST. The negative temperature effect on particle mass was slightly stronger in the high humidity experiments than in the low humidity ones. In general the volatility increased with increased relative humidity, demonstrating the important role humidity plays in product distribution (Figure 4.1, R3a). In theory, for the low humidity experiments, more of the low volatile secondary ozonide (R3b) could be formed with the

reaction of a carbonyl, e.g. by the formation of nopinone via R1a. However Docherty and Ziemann (2003) have shown this pathway does not contribute to SOA formation.

The inconsistencies in β -pinene ozonolysis may be explained by an alternative reaction pathway. In paper I, we suggest that the C₉-SCI (R2a) can rearrange into a hydroperoxide, something previously suggested by (Drozd and Donahue 2011; Nguyen et al. 2009; Zhang and Zhang 2005). This would favour the hydroperoxide channel, illustrated in Figure 4.3. This pathway explains the scavenger effect, producing more volatile particles under high HO₂/RO₂ ratios, as the radical chain can be terminated by HO₂. It also explains the relative humidity effect, since it would compete with the reaction between C₉-SCI and water (R3a) forming the highly volatile compound nopinone.

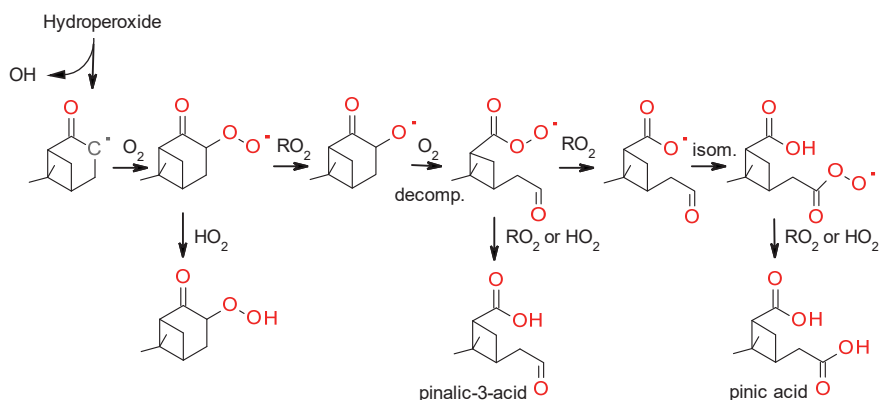


Figure 4.3 Formation of multifunctional oxygenated products by a sequence of radical reactions of β -pinene, starting with the alkyl radical from the hydroperoxide channel shown in Figure 4.1.

In paper II, the formation of dimer esters from the oxidation of α -pinene, generated in G-FROST, was studied using Ultra-High-Performance Liquid Chromatography/Mass Spectrometry (UHPLC/MS). The results elucidated the effects of ozone and OH-initiated oxidation, humidity and radical chemistry on α -pinene dimer formation. The concentration of dimer esters from α -pinene in the particle phase were much higher during ozonolysis experiments with 2-butanol present as an OH scavenger, than in OH oxidation, indicating that ozone is required for the initial formation of dimer esters. The initial steps of ozonolysis by α -pinene suggested in paper II are similar to those in β -pinene, consisting of gas-phase reactions forming a SCI. The SCI in turn reacts with oxygenated organics, resulting in the formation of dimer esters, as shown in Figure 4.2.

The dimer esters considered in paper II, having a low p_s , contributed significantly (~5–16%) to SOA formed from α -pinene oxidation. The dimer esters were not detected in the gas phase, probably due to their low volatility and therefore low concentration in the gas phase. Mohr et al. (2017) have since detected dimers in the gas phase in Hyytiälä with a FIGAERO-ToF-CIMS and their presence has also been confirmed by lab studies (Zhang et al. 2017). This supports the hypothesis that the reactions take place in the gas phase. Moreover, some of the 28 dimer esters detected in paper II were found in very high concentrations in the particle phase, in some cases even greater than some of the first-generation products from ozonolysis by α -pinene. This observation, combined with the short reaction times in G-FROST, indicates that dimer esters form quickly and are thus important for new particle formation.

In paper II, the ozonolysis experiments with α -pinene under humid conditions yielded the highest fraction of dimer esters in SOA. In the presence of OH-scavenger, the fraction of dimer esters in SOA was a few percent higher than that for the experiments without a scavenger (under humid conditions). In the humid experiments with OH-scavenger, the eight most abundant dimer esters increase by 60% compared with the results for experiments that did not use a scavenger. The majority of the other dimer esters (20 of 28) were more abundant in SOA under humid conditions when no OH-scavenger was present, indicating the scavenger suppressed formation of those dimer esters. For the experiments under dry conditions, the presence of an OH-scavenger yielded fewer dimer esters than experiments without a scavenger. For both dry experiments, the same eight dimer esters as for the humid experiments were responsible for the majority (approximately 70-80%) of the dimer esters in SOA. For the dry experiment with scavenger, the same suppressing effect on the 20 dimers was observed.

These results indicate that the formation of dimer esters requires ozonolysis for the initial oxidation steps of α -pinene. Furthermore, OH radicals enhance formation of some dimer esters, possibly via the RO₂ self-reaction. The results also indicate that both O₃ and OH oxidation is important for the formation of dimers in the atmosphere once the initial oxidation steps are finished. Similar results have been obtained in ambient air (Mohr et al. 2017). In addition, 15 of the 28 dimer esters found in the G-FROST experiments were also detected in Hyytiälä. The dimer esters from α -pinene comprised 1% of the total PM₁ in Hyytiälä. The dimer esters detected in Hyytiälä are from oxidation from α -pinene, suggesting the total fraction of dimer esters could be much higher since monoterpenes other than α -pinene and

and sesquiterpenes, have been detected in Hyytiälä (Hakola et al. 2012). Thus, This was later confirmed by Mohr et al. (2017) who found that up to 5% of the particle mass for particles smaller than 60nm in Hyytiälä were comprised of dimers, also demonstrating the importance of dimers during nucleation events.

4.2 Observations under ambient conditions

In order to better understand how particles behave in the atmosphere, three field studies were conducted. In Hyytiälä (paper III), at SOAS (paper IV) and Beijing (paper V), the gas and particle phases were continuously monitored. In Figure 4.4a the average gas signal (black) and particle signal (red) from one desorption in Hyytiälä are shown. The particle signal is shifted + 0.5amu in the interests of clarity. Detailed sections of the spectra are displayed in Figures 4.4b) and c). Figure 4.4b) displays some relevant acidic products from monoterpene oxidation, such as pinic acid (m/z 185) and pinonic acid (m/z 183). Figure 4.4c) displays highly oxidized acidic compounds. Figure 4.4 also shows that the ratio of the particle signal to gas signal increases with increasing molecular weight.

For the majority of compounds detected in particle phase in Hyytiälä, more than one desorption peak was obtained, as exemplified in Figure 3.6. The desorption peak at the lowest temperature was selected and further analyzed. The second desorption peak typically had a T_{\max} between 20-100 K higher than the first one, leading to the conclusion that they were thermally decomposed products from larger molecules, rather than isomers (Lopez-Hilfiker et al. 2015). For the same reason, when the particle signal was calculated, only the first desorption peak was integrated and considered for the partitioning calculations.

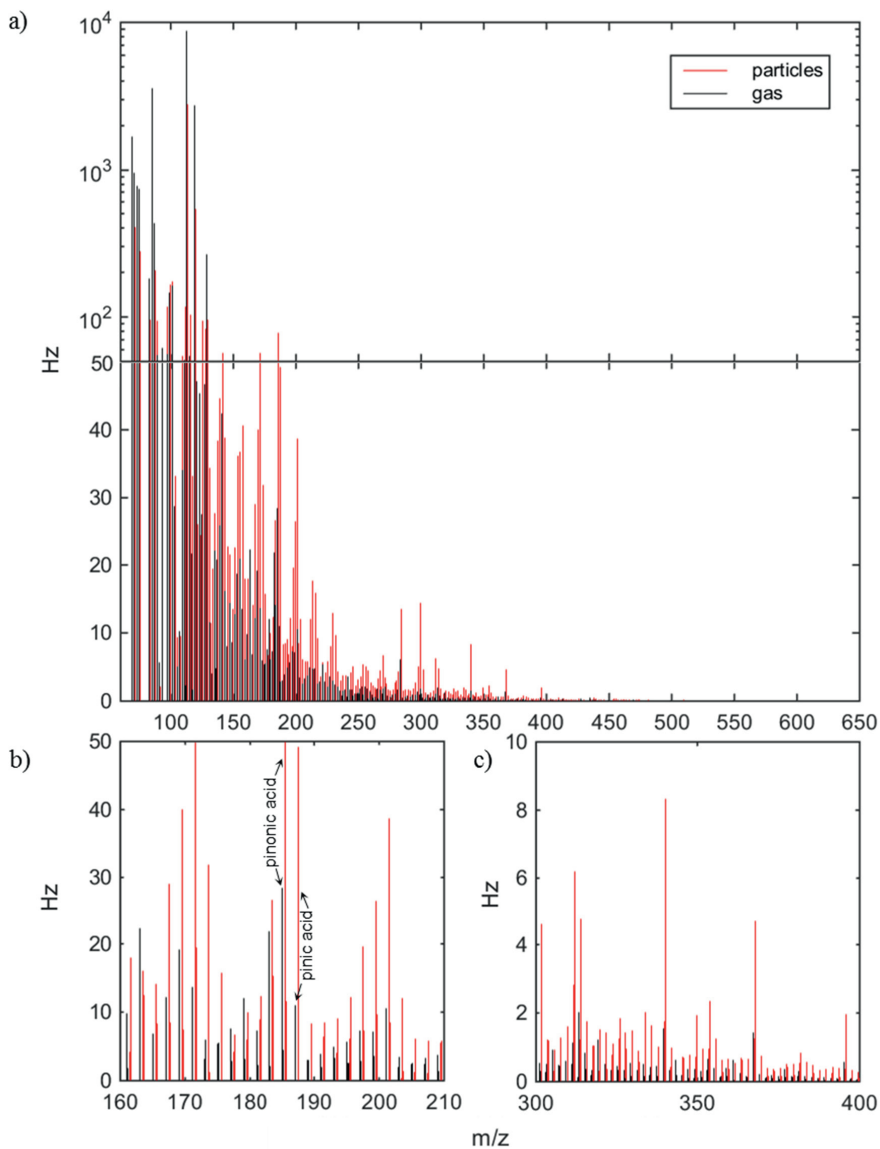


Figure 4. a) Example of a mass spectrum from Hyttiäla, Finland recorded with FIGAERO-ToF-CIMS with acetate as the reagent ion. The average gas signal is displayed in black. The average particle signal for one desorption sampled at the same time is shown in red and shifted $+0.5 \text{ amu}$ in the interests of clarity. b) Important acidic products from α -pinene oxidation, such as pinic acid (m/z 185) and pinonic acid (m/z 183) and c) Highly oxidized acidic compounds.

The maximum desorption temperatures (T_{\max}) for each compound detected in Hyytiälä (paper

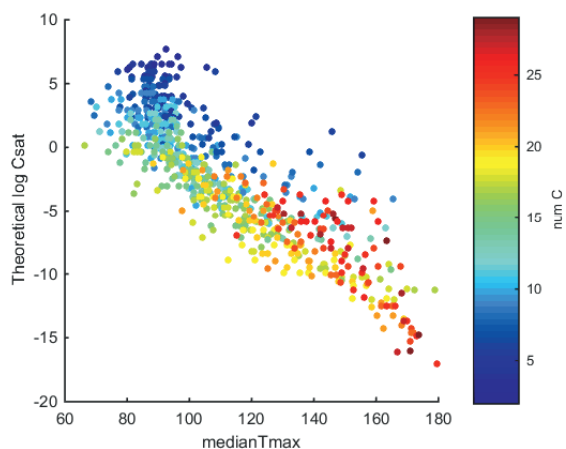


Figure 4.5 Median T_{\max} compared with the theoretical logarithmic saturation concentration (Donahue et al. 2011, Trostl et al. 2016)

III) were compared with the theoretical saturation concentration – predicted by Donahue et al. (2011) and revised by Trostl et al. (2016), as described in Section 2.3 – using each compound’s chemical formula rather than its structure. There is an exponential correlation between the theoretical saturation concentration and T_{\max} , as shown in Figure 4.5 (log scale), suggesting T_{\max} can indeed be used as a proxy for the theoretical saturation concentration.

Another interesting approach is to find a relationship between T_{\max} and the p_s of a series of polyethylene glycols ($\text{H}-(\text{O}-\text{CH}_2-\text{CH}_2)_n-\text{OH}$) which covers p_s over a large range (10^{-1} – 10^{-7} Pa) (Bannan et al. 2018). This enables the measured T_{\max} for unknown compounds to be calibrated and so estimate a saturation vapor pressure. Unfortunately the equation developed by Bannan et al. (2018) could not be used in this work as a FIGAERO inlet of different design, and therefore different heat losses, was used. Understanding the relationship between T_{\max} and p_s for the FIGAERO used in this work is outside the scope of this thesis but could be performed in the future.

The FIGAERO was deployed in the field for the first time during the measurements in Hyytiälä 2013, and its performance was evaluated by taking measurements of compounds previously detected in Hyytiälä. More extensive tests of the performance of FIGAERO were conducted in the lab, such as gas transmission, particle collection efficiency, and gas adsorption to the filter, described by Lopez-Hilfiker et al. (2014). Since pinic and pinonic acid are expected to be the major oxidation products from monoterpenes (Kristensen et al. 2016; Yatavelli et al. 2014; Zhang et al. 2010), it was assumed that the ions $\text{C}_{10}\text{H}_{15}\text{O}_3^-$ and $\text{C}_9\text{H}_{13}\text{O}_4^-$ were pinonic and pinic acid, respectively. These two oxidation products were investigated in detail in order to evaluate the accuracy of the FIGAERO- ToF-CIMS. Bilde and Pandis

(2001) established that pinic acid has a lower p_s than pinonic acid, in line with our results, where the fraction of pinonic acid in the particle phase is much lower than the fraction of pinic acid, as shown in Figure 1 of paper III. A previous study, measuring pinic and pinonic acid in Hyytiälä in both gas and particle phase obtained higher gas phase concentrations and lower particle phase concentrations (Kristensen et al. 2016). The difference in concentrations was attributed to the two sets of measurements being performed at different times of the year (resulting in lower ambient temperatures when our measurements were recorded), yielding different emission patterns of the precursors (Hakola et al. 2003). However, both studies measured a higher fraction of pinic acid in the particle phase, compared with pinonic acid, illustrating the effect of p_s on partitioning.

The simultaneous gas and particle phase measurements were conducted every 1 to 2 hours, which is relatively frequent in comparison with other methods, which normally have a much longer time resolution and detect only a few compounds. An analysis of the results obtained in Hyytiälä (paper III) showed that partitioning between compounds by the ideal partitioning theory, i.e. Raoult's law, can be applied in the ambient atmosphere under some conditions. Partitioning coefficients for over 640 organic acids were obtained with the FIGAERO-CIMS in Hyytiälä. However, whenever there is anthropogenic influence, as indicated by high SO_4^{2-} concentrations in the particle phase, the calculated partitioning coefficient deviates significantly for the most and least volatile compounds.

From equation 2.1, K_i is predicted to increase as p_s decreases: i.e. more of each compound will be found in the particle phase when the p_s decreases. Figure 4.5 shows a linear correlation between the saturation concentration and median T_{max} in Hyytiälä, illustrating that T_{max} can be used as a proxy for the p_s in the field as well as in the lab (Bannan et al. 2018). From the correlation with T_{max} , the partitioning coefficient, K_i , is expected to increase with increasing T_{max} , since a larger K_i corresponds to more material in the particle phase. However, this correlation was not observed in the data from Hyytiälä nor from the similar data from Beijing. Here K_i for each compound was calculated from the derived slope of the curve obtained for gas to particle ratio versus organic mass, from the whole measurement campaign. The quality of each linear fit was determined by the coefficient of determination (R^2), as exemplified in Figure 4.6.

NOT FOR PUBLIC RELEASE

NOT FOR PUBLIC RELEASE

NOT FOR PUBLIC RELEASE

NOT FOR PUBLIC RELEASE

Figure 4.6 Examples of particle to gas signal ratios plotted against organic mass from Hyytiälä. Circles: all data, filled circles: low sulfate concentration ($\text{SO}_4^{2-} < 0.4 \mu\text{g}/\text{m}^3$). Left: Pinonic acid. Right: The dimer, $\text{C}_{16}\text{H}_{21}\text{O}_6^-$, identified by Mohr et al, 2017. The solid line is the linear fit to the data with low sulfate concentration ($\text{SO}_4^{2-} < 0.4 \mu\text{g}/\text{m}^3$). The dashed line is the linear fit for data with high sulfate concentration ($\text{SO}_4^{2-} \geq 0.4 \mu\text{g}/\text{m}^3$).

Figure 4.6 reveals that the correlation between the particle/gas signal ratio to M_{org} (aerosol organic mass concentration) is rather low. Further investigation showed that the correlation did not improve by correlating the particle/gas signal ratio to particle size distributions, new particle formation events, relative humidity, ambient temperature, nitrate or ammonium content in $\text{PM}_{2.5}$. However, in Hyytiälä for clean air masses, defined as air masses with low sulfate particle concentration ($\text{SO}_4^{2-} < 0.4 \mu\text{g}/\text{m}^3$), the value of R^2 was considerably higher than for episodes affected by anthropogenic and aged air masses ($\text{SO}_4^{2-} > 0.4 \mu\text{g}/\text{m}^3$). A similar sulfate effect was also seen in Beijing, although the increase in the value of R^2 occurred at somewhat higher sulfate concentrations, and was not as pronounced, as illustrated in Figure 4.7. In Hyytiälä, the SO_4^{2-} concentration range was 0.1–1.6 $\mu\text{g}/\text{m}^3$, and the organic mass range was 0.2–2.0 $\mu\text{g}/\text{m}^3$. The SO_4^{2-} concentration range in Beijing was 0.25–16.0 $\mu\text{g}/\text{m}^3$ and organic mass range was 0.6–26.0 $\mu\text{g}/\text{m}^3$. In Hyytiälä, when the sulfate concentration was low, K_i increased with increasing T_{max} in accordance with equation 2.1. The effect of the origin of the air mass on K_i was especially pronounced for compounds with high and low T_{max} , i.e. higher and lower volatility compounds. K_i was not influenced by the ambient relative humidity, therefore it is unlikely that it is the concentration of sulfate, which is highly dependent on humidity, that causes a change in K_i . The effect on K_i is more likely to be linked to other properties of the aerosol that change during high sulfate episodes. One possible explanation

for this could be that the activity coefficient, γ , is larger during high SO_4^{2-} episodes. For the periods of high sulfate, K_i is generally lower for larger compounds. This could be because some larger compounds, such as larger acids, are known to have a higher activity coefficient (Cappa et al. 2008). Another factor that may affect the partitioning is viscosity. If the SOA are in an amorphous solid state or highly viscous, there would be kinetic limitations of diffusion to the bulk of the particles (Virtanen et al. 2010). This could be the result of higher viscosity in the particle phase during high levels of SO_4^{2-} .



Figure 4.7 Coefficient of determination, R^2 , for particle/gas signal versus organic particle mass. R^2 increases as the data points having high SO_4^{2-} are removed, as indicated by the threshold. The maximum sulfate concentration was $1.6 \mu\text{g}/\text{m}^3$ in Hyytiälä and $16 \mu\text{g}/\text{m}^3$ in Beijing.

For the Hyytiälä data, all the compounds for which there was a statistically significant relationship ($p < 0.05$) between their particle/gas ratio and M_{org} during the low sulfate conditions were analyzed further in order to elucidate the relationship between K_i and T_{max} . The compounds fulfilling this criterion are displayed in the Kendrick mass defect plot in Figure 4.8. The Kendrick mass defect plot is a useful tool to find compounds that differ by a base unit, in this case CH_2 , in a high resolution mass spectrum (Kendrick 1963). The plot displays the Kendrick mass on the X-axis, defined as the IUPAC mass multiplied by $14.00000/14.01565$, and, on the Y-axis, the Kendrick mass defect, calculated as the Kendrick mass subtracted from the integer mass (Kendrick 1963). In Figure 4.8, the circles represent the measured compounds and the color code represents the median T_{max} for each compound. The dotted lines are examples of where different molecules would appear. The magenta line

corresponds to a straight chain carboxylic acid, the red line to a straight line dicarboxylic acid and the black line to a dicarboxylic acid where each carbon outside the functional group is bound to oxygen. This plot shows that the majority of the compounds are more oxygenated than a carboxylic acid. In addition, some compounds, having one double bound oxygen molecule per carbon in a straight chained dicarboxylic acid, are shown as the dashed black line. The red dashed line shows where dicarboxylic acids with an alcohol (OH-group) bound to each carbon atom would end up. According to the definition by Tu et al. (2016) many of the compounds detected in Hyytiälä are HOM, as indicated by the area above the green dashed line in Figure 4.8, showing compounds with $OS_C \geq 0$.

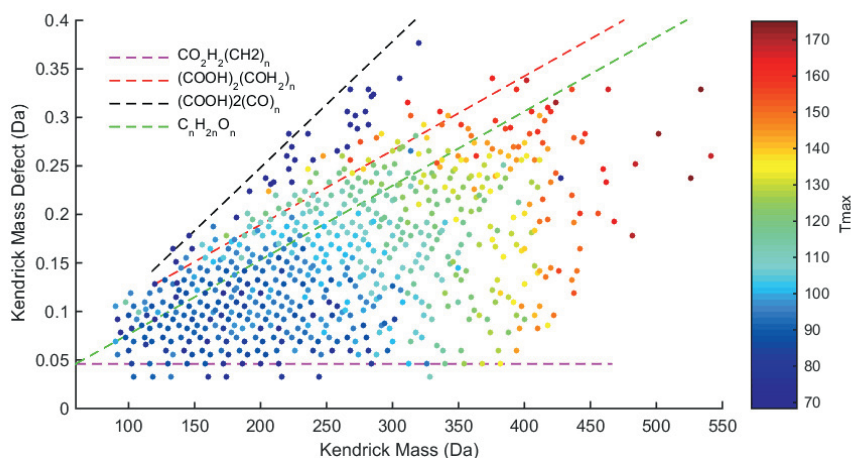


Figure 4.8 Kendrick mass defect plot for the compounds with p-values < 0.05 during low sulfate conditions. The circles are the measured compounds. The color code represents the median T_{max} for each compound. The lines are examples of where molecules would lie. The magenta line corresponds to a straight chain carboxylic acid, the red line to a straight line dicarboxylic acid, the black to a dicarboxylic acid for which each carbon outside the acid functional group is a carbonyl ($C=O$) and the green line represents a molecule having a $OS_C = 0$.

In China, severe pollution in the large cities is a major threat to the health of their inhabitants. The pollution also threatens the economy and the government strives to reduce primary emissions. How this will affect secondary pollutants is unclear. For example the London smog, which occurred during winter due to a combination of cold weather and increased coal burning, was caused by sulfur dioxide and soot being trapped by temperature inversion. Summertime smog – as occurs in e.g. Los Angeles – is caused by VOCs and nitrogen oxides reacting with sun light, i.e. photochemical smog. Both these types of smog occur in China,

including pollution of ozone, soot, sulfur dioxide, VOCs, NO_x and organic particles. Thus actions to reduce pollution in China cannot be based solely on what has been done to improve air quality in the US and Europe (Hallquist et al. 2016).

The conditions in Changping, near Beijing, were very different from Hyytiälä. The sulfate effect on partitioning is seen in Figure 4.7, but here the sulfate concentration in the particles is much higher. The much lower correlation coefficients in Changping are most likely partly due to the signal to noise ratio in Changping being much lower than it was in Hyytiälä. The reason for this was not being able to use ²¹⁰Po to produce the reagent ion in China. Instead, an X-ray source was used for ionizing in the production of the reagent ion, which, unfortunately, yielded a much lower total ion-count. The air in Changping was always affected by anthropogenic influence as the wind direction always came from the southerly sectors (90-270°). Two distinct regimes of air pollution were discovered: one when the wind came from the south-east, where Beijing is located; the other when the wind came from the south-west, which was more influenced by forest and farming emissions.

Figure 4.9 displays core data from the campaign in Changping. The anthropogenic tracer SO₄²⁻ in the particle phase comes mainly from the south-east. The majority of the organic mass also comes from the south-east, meaning that it is highly influenced by industry and traffic, as is seen from the wind rose for benzene. In the air masses from the south-west, being from more forested areas, isoprene occurred in the largest concentration. In addition, the maximum winds speed from the south-east was 3 m/s and 6 m/s from the south-west, suggesting a short range transport and hence local contribution. The lower signal to noise ratio for the ToF-CIMS measurements taken in Changping, in combination with the lack of northerly winds bringing in cleaner air masses, complicated the interpretation of this dataset in relation to the Hyytiälä data. Thus, in order to further understand gas to particle partitioning in Changping, one would need more data, especially from the cleaner sector in the north where the air masses are more influenced by biogenic emissions.



Figure 4.9 Frequency of counts by wind direction, for organic mass and sulfate in particles, and for benzene and isoprene in gas phase.

However, the high sulfate concentrations in Beijing were used to study the behavior of dimers in particle phase in Changping. In Hyytiälä, a larger effect of sulfate was observed for compounds with higher T_{max} , indicative of dimers being more affected by sulfate than other compounds (Figure 4.7). The dimer particle signal in Changping was ordered by mass ranges, since no T_{max} could be extracted, and normalised to total particle signal. It was evident from these data that the number of dimers observed in the particle phase relative to the total particle signal decreased at higher sulfate concentrations. This reduction in signal relative to the total particle signal with increased sulfate is similar to other observations by Riva et al. (2019) in Hyytiälä for a smaller range in sulfate. This was also the case for another site in China, Dezhou, included to emphasise this effect also at high sulfate concentration. We could also observe a sulfate effect on dimer concentration for the two Chinese sites and thus confirm the recent findings by Riva et al. (2019). Riva et al. (2019) also noticed an increase in compounds

having high molecular weight (greater than approximately 600 g/mol) with increasing sulfate concentration. In Changping no higher molecular weight (HMW) compounds could be measured due to the poor signal. The increase in HMW compounds indicates that the chemistry in the particles is changed with increased acidity, which is indicated by sulfate concentration. Oligomers have previously been observed to form in the particle phase (Hall and Johnston 2012). However, the fact that the measured monomer concentration in the particle phase did not increase with increased monomer gas concentration suggests that the formation of oligomers is driven by reactive uptake in the particle phase rather than by equilibrium partitioning (Hall and Johnston 2012).

During the SOAS campaign in Centreville, Alabama (paper IV), 88 organic nitrates (ON) were identified in the particle phase. During the day (12:00–16:00) they contributed 3%, on average, to the total organic mass measured by the AMS, while during the night (22:00–05:00) they contributed 8%, on average. The measurements of particle organic nitrates (pON) using FIGAERO-ToF-CIMS agreed well with measurements taken using two AMS instruments operating in parallel. The measurements obtained from a thermal dissociation laser induced fluorescence (TD-LIF) instrument followed the same trends as our measurements, but were around a factor of 5 higher in concentration. However, all instruments displayed a diurnal pattern with higher concentrations of pON during the night than the day.

In order to investigate the effect of monoterpenes (C_{10}) and isoprene (C_5) precursors on pON, the pON were divided into two groups having 5 and 10 carbon atoms, respectively. The fraction of pONs with 10 and 5 carbons over the sum of pONs with C_{10} and C_5 groups, show an opposite diurnal trend, consistent with the average levels of their precursors, isoprene and monoterpenes, as shown by Figure 4.10. The fraction of C_5 pON follows the same pattern as isoprene, and the diurnal patterns for C_{10} pON follow the same pattern as the monoterpenes. This strongly suggests that the pON processes occur on a timescale of a few hours. A potential reason for such a fast gas phase reaction followed by loss to particle phase could be oxidation by OH (George and Abbatt 2010).

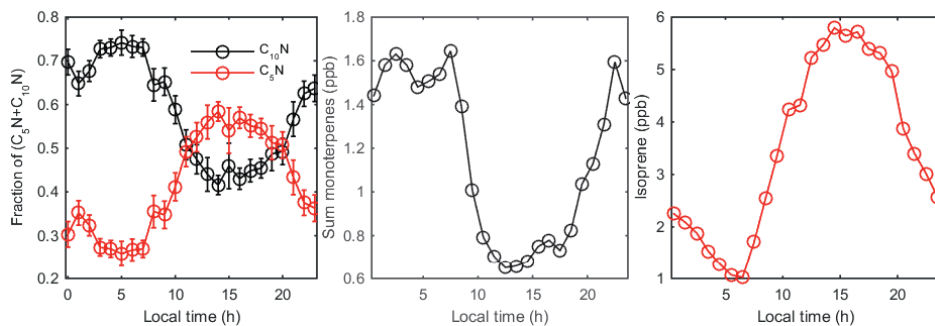


Figure 4.10 Particle organic nitrates (pON) and their precursors. Left: Fraction of pON originating from C_{10} and C_5 , over the sum of the C_{10} and C_5 groups. Middle: Sum of monoterpenes varying over the day. Right: Diurnal isoprene pattern.

The dominant molecular composition of the pON discussed in paper IV is of monoterpenes and isoprene that were more oxygenated than previously reported, with each pON having between 4-11 oxygens. The number of oxygens in a compound lowers the p_s , meaning that the compound will partition to the particle phase to a larger extent. Previously, highly oxygenated molecules were detected in the laboratory (Ehn et al. 2014; Jokinen et al. 2015). In paper IV, we report the first observations in the field of highly oxidised pON. The pON contributed 3%, on average, to the organic mass, but the measurements from the TD-LIF, suggests the fraction of pON in organic aerosols could be even higher.

5. Atmospheric implications

In the ambient atmosphere a myriad of reactions take place simultaneously. Predicting future SOA concentrations and composition of aerosols in a warmer climate is challenging: SOA formation is affected by increased temperature in several different ways, including higher VOC emissions, faster reaction rates and decreased partitioning from gas into particle phase (Tsigaridis and Kanakidou 2007). In addition, oligomerization/accretion processes of compounds within particles, predicted to occur when the aerosol particles are more acidic (Riva et al. 2019), makes the particles less volatile and therefore affects their lifetime (Shrivastava et al. 2017).

The work described in this thesis investigated partitioning between gas and particles, particle volatility and particle composition in detail. In papers I and II, the formation of SOA was studied in a controlled laboratory environment. The results revealed that β -pinene produces fewer particles as humidity increases. The paper also suggests a new mechanistic pathway explaining the effect on relative humidity. For α -pinene, ozonolysis, not OH, is important for the initial step in dimer ester formation. These findings make an important contribution to the understanding of the underlying chemical reactions and improve our ability to predict the influence of SOA on the climate and air quality in the future (Burkholder et al. 2017).

Partitioning between gas and particle phase in the atmosphere, in some cases, can be described by Raoult's law, as shown in papers III and V. The level of anthropogenic influence is a key factor in this partitioning. In order to model the mass of SOA and predict the impact SOA will have on society, accurate models of SOA formation are needed. The basis for such models includes knowledge of gas to particle partitioning and the factors that influence this partitioning. In addition, knowledge of the compounds in the particles is needed. Traditionally, volatility has been assumed to be the parameter that governs partitioning (Donahue et al. 2011), but partitioning between gas and particle phases is also affected by other processes, which new models of organic aerosol formation should consider. Examples of such processes are reactions in the bulk of the particles, the formation of high molecular weight compounds from oligomers which is affected by the inorganic composition or acidity (Riva et al. 2019). Presumably, new models should also take particle-phase processing and the (previously underestimated) importance of inorganic components in SOA formation into account.

Paper IV demonstrated that highly oxidized pON are formed from oxidation of BVOCs when NO_x is present. Thus, pON formation can enhance gas to particle partitioning for compounds of intermediate volatility in regions with elevated concentrations of NO_x via their contribution to increased organic mass (Ng et al. 2007). In addition, ON formed from isoprene are estimated to remove 8–30% of the anthropogenic NO_x in the USA (Horowitz et al. 1998; Liang et al. 1998), meaning a change in gas to particle partitioning could affect the amount of gaseous NO_x in those areas significantly.

To conclude, the work described in this thesis has improved the understanding of the chemical composition and gas to particle partitioning of SOA. The FIGAERO- ToF-CIMS was used to elucidate the composition of an aerosol in the particle and gas phases, making it possible to learn more about gas to particle partitioning. It was revealed that Raoult's law can be used to predict gas to particle partitioning in cases when the anthropogenic pollution is low. It was also revealed that volatility is not the sole component that drives partitioning; the inorganic content or the acidity, or potentially both, of the particles are also important.

Acknowledgements

"I was taught that the way of progress was neither swift nor easy." – Marie Curie, physicist, chemist, and winner of the 1903 and the 1911 Nobel Prize in Physics.

Being a PhD student requires a lot of hard work, but it is also a lot of fun! Many people have contributed to making my time as a PhD student happy. First of all I would like to acknowledge my supervisor Professor Mattias Hallquist for giving me this opportunity and for always pushing me. You are a great scientist! You always see the new opportunities when things do not go as expected. I would also like to acknowledge my assistant supervisors, Assistant Professor Claudia Mohr and Dr. Mike Le Breton, for helping me with data analysis and always being available to discuss data and results. Claudia, you were a great host during my visits to the US and you helped me a great deal with Matlab. Mike, you are a truly nice guy and it was always fun talking to you. I would also like to acknowledge Professor Emeritus Evert Ljungström, for being my assistant supervisor until he retired. I do not think I ever presented a problem to you that you could not solve. My thanks go to my examiner Professor Jan Pettersson for fruitful discussions about my research as well as private matters. Thanks also go to Professor Johan Boman for checking up on me and for reading my thesis and asking the “hard to solve” questions. I am really thankful to Dr. Mike Priestley for his help during my final weeks, I am so grateful and impressed by your skills! Dr. Christian Mark Salvador, thanks for all the help and for cheering me up in the late hours at the office. I am also very grateful to everyone participating in the field campaigns that I attended during my years as a student.

Atmochicks are acknowledged for excellent friendship, in an otherwise male dominated environment. Ågot, you are a great scientist and my SOA soul mate, always up for discussing science and other things too! Sofia, thanks for always supporting me, you made my days in the group really fun. Julia, it was great learning about the CIMS (and Walmart, and outlets and.... a lot more) with you, Lebkuchen FTW. Sam is acknowledged according to clause 2.5, office agreement for being an awesome office mate. Eva, thanks for introducing me to atmospheric science via G-FROST and also for introducing me to the flea markets of Gothenburg and Alebacken! I am very grateful to every former and current member of the Atmospheric Science group for making it fun to be at work!

Finally, I am very grateful to my entire family and all my friends. I would not have made it without you. Nils, you are really smart and funny and I am very proud of you. You always make me think about other things than work when I am home. To my husband, Martin: thanks for taking more than your share during the last months! I love you <3. I am also very grateful to my mom for helping us with Nils: without you our lives would be even more chaotic! I also acknowledge the Swedish school system for my free education, and for taking care of my child when I am at work. All personnel at the preschool “Just Like Hemma” are acknowledged, for being understanding and for being such great teachers. It is easier for me to work when I know that Nils is well looked after.

References

- Atkinson, R., and Arey, J. (2003). "Atmospheric Degradation of Volatile Organic Compounds." *Chemical Reviews*, 103(12), 4605-4638.
- Bannan, T. J., Le Breton, M., Priestley, M., Worrall, S. D., Bacak, A., Marsden, N. A., Merha, A., Hammes, J., Hallquist, M., Alfarra, M. R., Krieger, U. K., Reid, J. P., Jayne, J., Robinson, W., McFiggans, G., Coe, H., Percival, C. J., and Topping, D. (2018). "A method for extracting calibrated volatility information from the FIGAERO-HR-ToF-CIMS and its application to chamber and field studies." *Atmos. Meas. Tech. Discuss.*, 2018, 1-12.
- Bilde, M., Barsanti, K., Booth, M., Cappa, C. D., Donahue, N. M., Emanuelsson, E. U., McFiggans, G., Krieger, U. K., Marcolli, C., Topping, D., Ziemann, P., Barley, M., Clegg, S., Dennis-Smith, B., Hallquist, M., Hallquist, A. M., Khlystov, A., Kulmala, M., Mogensen, D., Percival, C. J., Pope, F., Reid, J. P., da Silva, M., Rosenoern, T., Salo, K., Soonsin, V. P., Yli-Juuti, T., Prisle, N. L., Pagels, J., Rarey, J., Zardini, A. A., and Riipinen, I. (2015). "Saturation Vapor Pressures and Transition Enthalpies of Low-Volatility Organic Molecules of Atmospheric Relevance: From Dicarboxylic Acids to Complex Mixtures." *Chemical Reviews*, 115(10), 4115-4156.
- Bilde, M., and Pandis, S. N. (2001). "Evaporation rates and vapor pressures of individual aerosol species formed in the atmospheric oxidation of alpha- and beta-pinene." *Environmental Science & Technology*, 35(16), 3344-3349.
- Borbon, A., Gilman, J. B., Kuster, W. C., Grand, N., Chevaillier, S., Colomb, A., Dolgorouky, C., Gros, V., Lopez, M., Sarda-Estevé, R., Holloway, J., Stutz, J., Petetin, H., McKeen, S., Beekmann, M., Warneke, C., Parrish, D. D., and de Gouw, J. A. (2013). "Emission ratios of anthropogenic volatile organic compounds in northern mid-latitude megacities: Observations versus emission inventories in Los Angeles and Paris." *Journal of Geophysical Research-Atmospheres*, 118(4), 2041-2057.
- Burkholder, J. B., Abbatt, J. P. D., Barnes, I., Roberts, J. M., Melamed, M. L., Ammann, M., Bertram, A. K., Cappa, C. D., Carlton, A. G., Carpenter, L. J., Crowley, J. N., Dubowski, Y., George, C., Heard, D. E., Herrmann, H., Keutsch, F. N., Kroll, J. H., McNeill, V. F., Ng, N. L., Nizkorodov, S. A., Orlando, J. J., Percival, C. J., Picquet-Varraut, B., Rudich, Y., Seakins, P. W., Surratt, J. D., Tanimoto, H., Thornton, J. A., Tong, Z., Tyndall, G. S., Wahner, A., Weschler, C. J., Wilson, K. R., and Ziemann, P. J. (2017). "The Essential Role for Laboratory Studies in Atmospheric Chemistry." *Environmental Science & Technology*, 51(5), 2519-2528.
- Cappa, C. D., Lovejoy, E. R., and Ravishankara, A. R. (2008). "Evidence for liquid-like and nonideal behavior of a mixture of organic aerosol components." *Proceedings of the National Academy of Sciences of the United States of America*, 105(48), 18687-18691.
- Carlton, A. G., de Gouw, J., Jimenez, J. L., Ambrose, J. L., Attwood, A. R., Brown, S., Baker, K. R., Brock, C., Cohen, R. C., Edgerton, S., Farkas, C. M., Farmer, D., Goldstein, A. H., Gratz, L., Guenther, A., Hunt, S., Jaegle, L., Jaffe, D. A., Mak, J., McClure, C., Nenes, A., Nguyen, T. K., Pierce, J. R., de Sa, S., Selin, N. E., Shah, V., Shaw, S., Shepson, P. B., Song, S. J., Stutz, J., Surratt, J. D., Turpin, B. J., Warneke, C., Washenfelder, R. A., Wennberg, P. O., and Zhou, X. L. (2018). "Synthesis of the

- southeast atmosphere studies: Investigating Fundamental Atmospheric Chemistry Questions." *Bulletin of the American Meteorological Society*, 99(3), 547-567.
- Compernelle, S., Ceulemans, K., and Muller, J. F. (2011). "EVAPORATION: a new vapour pressure estimation method for organic molecules including non-additivity and intramolecular interactions." *Atmospheric Chemistry and Physics*, 11(18), 9431-9450.
- Docherty, K. S., Wu, W., Lim, Y. B., and Ziemann, P. J. (2005). "Contributions of organic peroxides to secondary aerosol formed from reactions of monoterpenes with O₃." *Environmental Science & Technology*, 39(11), 4049-4059.
- Docherty, K. S., and Ziemann, P. J. (2003). "Effects of stabilized Criegee intermediate and OH radical scavengers on aerosol formation from reactions of beta-pinene with O₃." *Aerosol Science and Technology*, 37(11), 877-891.
- Donahue, N. M., Epstein, S. A., Pandis, S. N., and Robinson, A. L. (2011). "A two-dimensional volatility basis set: 1. organic-aerosol mixing thermodynamics." *Atmospheric Chemistry and Physics*, 11(7), 3303-3318.
- Drozd, G. T., and Donahue, N. M. (2011). "Pressure Dependence of Stabilized Criegee Intermediate Formation from a Sequence of Alkenes." *Journal of Physical Chemistry A*, 115(17), 4381-4387.
- Ehn, M., Kleist, E., Junninen, H., Petaja, T., Lonn, G., Schobesberger, S., Dal Maso, M., Trimborn, A., Kulmala, M., Worsnop, D. R., Wahner, A., Wildt, J., and Mentel, T. F. (2012). "Gas phase formation of extremely oxidized pinene reaction products in chamber and ambient air." *Atmospheric Chemistry and Physics*, 12(11), 5113-5127.
- Ehn, M., Thornton, J. A., Kleist, E., Sipila, M., Junninen, H., Pullinen, I., Springer, M., Rubach, F., Tillmann, R., Lee, B., Lopez-Hilfiker, F., Andres, S., Acir, I. H., Rissanen, M., Jokinen, T., Schobesberger, S., Kangasluoma, J., Kontkanen, J., Nieminen, T., Kurten, T., Nielsen, L. B., Jorgensen, S., Kjaergaard, H. G., Canagaratna, M., Dal Maso, M., Berndt, T., Petaja, T., Wahner, A., Kerminen, V. M., Kulmala, M., Worsnop, D. R., Wildt, J., and Mentel, T. F. (2014). "A large source of low-volatility secondary organic aerosol." *Nature*, 506(7489), 476+.
- Emanuelsson, E. U., Hallquist, M., Kristensen, K., Glasius, M., Bohn, B., Fuchs, H., Kammer, B., Kiendler-Scharr, A., Nehr, S., Rubach, F., Tillmann, R., Wahner, A., Wu, H. C., and Mentel, T. F. (2013a). "Formation of anthropogenic secondary organic aerosol (SOA) and its influence on biogenic SOA properties." *Atmospheric Chemistry and Physics*, 13(5), 2837-2855.
- Emanuelsson, E. U., Watne, A. K., Lutz, A., Ljungstrom, E., and Hallquist, M. (2013b). "Influence of Humidity, Temperature, and Radicals on the Formation and Thermal Properties of Secondary Organic Aerosol (SOA) from Ozonolysis of beta-Pinene." *Journal of Physical Chemistry A*, 117(40), 10346-10358.
- Finlaysson-Pitts, B. J., Pitts, J.N (2000). *Chemistry of the Upper and Lower Atmosphere Theory, Experiments, and Applications*, San Diego, California, USA: Academic Press.
- Fisher, J. A., Jacob, D. J., Travis, K. R., Kim, P. S., Marais, E. A., Miller, C. C., Yu, K. R., Zhu, L., Yantosca, R. M., Sulprizio, M. P., Mao, J. Q., Wennberg, P. O., Crounse, J.

- D., Teng, A. P., Nguyen, T. B., St Clair, J. M., Cohen, R. C., Romer, P., Nault, B. A., Wooldridge, P. J., Jimenez, J. L., Campuzano-Jost, P., Day, D. A., Hu, W. W., Shepson, P. B., Xiong, F. L. Z., Blake, D. R., Goldstein, A. H., Misztal, P. K., Hanisco, T. F., Wolfe, G. M., Ryerson, T. B., Wisthaler, A., and Mikoviny, T. (2016). "Organic nitrate chemistry and its implications for nitrogen budgets in an isoprene- and monoterpene-rich atmosphere: constraints from aircraft (SEAC(4)RS) and ground-based (SOAS) observations in the Southeast US." *Atmospheric Chemistry and Physics*, 16(9), 5969-5991.
- George, C., Ammann, M., D'Anna, B., Donaldson, D. J., and Nizkorodov, S. A. (2015). "Heterogeneous Photochemistry in the Atmosphere." *Chemical Reviews*, 115(10), 4218-4258.
- George, I. J., and Abbatt, J. P. D. (2010). "Heterogeneous oxidation of atmospheric aerosol particles by gas-phase radicals." *Nature Chemistry*, 2(9), 713-722.
- Goldstein, A. H., and Galbally, I. E. (2007). "Known and unexplored organic constituents in the earth's atmosphere." *Environmental Science & Technology*, 41(5), 1514-1521.
- Guenther, A. (1997). "Seasonal and spatial variations in natural volatile organic compound emissions." *Ecological Applications*, 7(1), 34-45.
- Guenther, A. B., Jiang, X., Heald, C. L., Sakulyanontvittaya, T., Duhl, T., Emmons, L. K., and Wang, X. (2012). "The Model of Emissions of Gases and Aerosols from Nature version 2.1 (MEGAN2.1): an extended and updated framework for modeling biogenic emissions." *Geoscientific Model Development*, 5(6), 1471-1492.
- Hakola, H., Hellen, H., Hemmila, M., Rinne, J., and Kulmala, M. (2012). "In situ measurements of volatile organic compounds in a boreal forest." *Atmospheric Chemistry and Physics*, 12(23), 11665-11678.
- Hakola, H., Tarvainen, V., Laurila, T., Hiltunen, V., Hellen, H., and Keronen, P. (2003). "Seasonal variation of VOC concentrations above a boreal coniferous forest." *Atmospheric Environment*, 37(12), 1623-1634.
- Hall, W. A., and Johnston, M. V. (2012). "Oligomer Formation Pathways in Secondary Organic Aerosol from MS and MS/MS Measurements with High Mass Accuracy and Resolving Power." *Journal of the American Society for Mass Spectrometry*, 23(6), 1097-1108.
- Hallquist, M., Munthe, J., Hu, M., Wang, T., Chan, C. K., Gao, J., Boman, J., Guo, S., Hallquist, A. M., Mellqvist, J., Moldanova, J., Pathak, R. K., Pettersson, J. B. C., Pleijel, H., Simpson, D., and Thynell, M. (2016). "Photochemical smog in China: scientific challenges and implications for air-quality policies." *National Science Review*, 3(4), 401-403.
- Hallquist, M., Wenger, J. C., Baltensperger, U., Rudich, Y., Simpson, D., Claeys, M., Dommen, J., Donahue, N. M., George, C., Goldstein, A. H., Hamilton, J. F., Herrmann, H., Hoffmann, T., Iinuma, Y., Jang, M., Jenkin, M. E., Jimenez, J. L., Kiendler-Scharr, A., Maenhaut, W., McFiggans, G., Mentel, T. F., Monod, A., Prevot, A. S. H., Seinfeld, J. H., Surratt, J. D., Szmigielski, R., and Wildt, J. (2009). "The

- formation, properties and impact of secondary organic aerosol: current and emerging issues." *Atmospheric Chemistry and Physics*, 9(14), 5155-5236.
- Hansen, D. A., Edgerton, E. S., Hartsell, B. E., Jansen, J. J., Kandasamy, N., Hidy, G. M., and Blanchard, C. L. (2003). "The southeastern aerosol research and characterization study: Part 1-overview." *Journal of the Air & Waste Management Association*, 53(12), 1460-1471.
- Hari, P., and Kulmala, M. (2005). "Station for measuring ecosystem-atmosphere relations (SMEAR II)." *Boreal Environment Research*, 10(5), 315-322.
- Hinds, W. C. (1998). *Aerosol Technology: Properties, Behavior, and Measurements of Airborne Particles*, New York: John Wiley & Sons.
- Horowitz, L. W., Liang, J. Y., Gardner, G. M., and Jacob, D. J. (1998). "Export of reactive nitrogen from North America during summertime: Sensitivity to hydrocarbon chemistry." *Journal of Geophysical Research-Atmospheres*, 103(D11), 13451-13476.
- Jimenez, J. L., Canagaratna, M. R., Donahue, N. M., Prevot, A. S. H., Zhang, Q., Kroll, J. H., DeCarlo, P. F., Allan, J. D., Coe, H., Ng, N. L., Aiken, A. C., Docherty, K. S., Ulbrich, I. M., Grieshop, A. P., Robinson, A. L., Duplissy, J., Smith, J. D., Wilson, K. R., Lanz, V. A., Hueglin, C., Sun, Y. L., Tian, J., Laaksonen, A., Raatikainen, T., Rautiainen, J., Vaattovaara, P., Ehn, M., Kulmala, M., Tomlinson, J. M., Collins, D. R., Cubison, M. J., Dunlea, E. J., Huffman, J. A., Onasch, T. B., Alfarra, M. R., Williams, P. I., Bower, K., Kondo, Y., Schneider, J., Drewnick, F., Borrmann, S., Weimer, S., Demerjian, K., Salcedo, D., Cottrell, L., Griffin, R., Takami, A., Miyoshi, T., Hatakeyama, S., Shimono, A., Sun, J. Y., Zhang, Y. M., Dzepina, K., Kimmel, J. R., Sueper, D., Jayne, J. T., Herndon, S. C., Trimborn, A. M., Williams, L. R., Wood, E. C., Middlebrook, A. M., Kolb, C. E., Baltensperger, U., and Worsnop, D. R. (2009). "Evolution of Organic Aerosols in the Atmosphere." *Science*, 326(5959), 1525-1529.
- Jokinen, T., Berndt, T., Makkonen, R., Kerminen, V. M., Junninen, H., Paasonen, P., Stratmann, F., Herrmann, H., Guenther, A. B., Worsnop, D. R., Kulmala, M., Ehn, M., and Sipila, M. (2015). "Production of extremely low volatile organic compounds from biogenic emissions: Measured yields and atmospheric implications." *Proceedings of the National Academy of Sciences of the United States of America*, 112(23), 7123-7128.
- Jonsson, A. M., Hallquist, M., and Ljungstrom, E. (2006). "Impact of humidity on the ozone initiated oxidation of limonene, Delta(3)-carene, and alpha-pinene." *Environmental Science & Technology*, 40(1), 188-194.
- Jonsson, A. M., Hallquist, M., and Ljungstrom, E. (2008). "The effect of temperature and water on secondary organic aerosol formation from ozonolysis of limonene, Delta(3)-carene and alpha-pinene." *Atmospheric Chemistry and Physics*, 8(21), 6541-6549.
- Jonsson, A. M., Hallquist, M., and Saathoff, H. (2007). "Volatility of secondary organic aerosols from the ozone initiated oxidation of alpha-pinene and limonene." *Journal of Aerosol Science*, 38(8), 843-852.

- Kendrick, E. (1963). "A mass scale based on CH₂=14.0000 for high resolution mass spectrometry of organic compounds." *Analytical Chemistry*, 35(13), 2146-&.
- Keywood, M. D., Kroll, J. H., Varutbangkul, V., Bahreini, R., Flagan, R. C., and Seinfeld, J. H. (2004). "Secondary organic aerosol formation from cyclohexene ozonolysis: Effect of OH scavenger and the role of radical chemistry." *Environmental Science & Technology*, 38(12), 3343-3350.
- Kim, K. H., Kabir, E., and Kabir, S. (2015). "A review on the human health impact of airborne particulate matter." *Environment International*, 74, 136-143.
- Kristensen, K., Bilde, M., Aalto, P. P., Petaja, T., and Glasius, M. (2016). "Denuder/filter sampling of organic acids and organosulfates at urban and boreal forest sites: Gas/particle distribution and possible sampling artifacts." *Atmospheric Environment*, 130, 36-53.
- Kroll, J. H., Donahue, N. M., Jimenez, J. L., Kessler, S. H., Canagaratna, M. R., Wilson, K. R., Altieri, K. E., Mazzoleni, L. R., Wozniak, A. S., Bluhm, H., Mysak, E. R., Smith, J. D., Kolb, C. E., and Worsnop, D. R. (2011). "Carbon oxidation state as a metric for describing the chemistry of atmospheric organic aerosol." *Nature Chemistry*, 3(2), 133-139.
- Kurten, T., Tiusanen, K., Roldin, P., Rissanen, M., Luy, J. N., Boy, M., Ehn, M., and Donahue, N. M. (2016). "alpha-Pinene Autoxidation Products May Not Have Extremely Low Saturation Vapor Pressures Despite High O:C Ratios." *Journal of Physical Chemistry A*, 120(16), 2569-2582.
- Le Breton, M., Wang, Y. J., Hallquist, A. M., Pathak, R. K., Zheng, J., Yang, Y. D., Shang, D. J., Glasius, M., Bannan, T. J., Liu, Q. Y., Chan, C. K., Percival, C. J., Zhu, W. F., Lou, S. R., Topping, D., Wang, Y. C., Yu, J. Z., Lu, K. D., Guo, S., Hu, M., and Hallquist, M. (2018). "Online gas- and particle-phase measurements of organosulfates, organosulfonates and nitrooxy organosulfates in Beijing utilizing a FIGAERO ToF-CIMS." *Atmospheric Chemistry and Physics*, 18(14), 10355-10371.
- Lee, B. H., Lopez-Hilfiker, F. D., Mohr, C., Kurten, T., Worsnop, D. R., and Thornton, J. A. (2014). "An Iodide-Adduct High-Resolution Time-of-Flight Chemical-Ionization Mass Spectrometer: Application to Atmospheric Inorganic and Organic Compounds." *Environmental Science & Technology*, 48(11), 6309-6317.
- Lefohn, A. S., Shadwick, D., and Oltmans, S. J. (2010). "Characterizing changes in surface ozone levels in metropolitan and rural areas in the United States for 1980-2008 and 1994-2008." *Atmospheric Environment*, 44(39), 5199-5210.
- Liang, J. Y., Horowitz, L. W., Jacob, D. J., Wang, Y. H., Fiore, A. M., Logan, J. A., Gardner, G. M., and Munger, J. W. (1998). "Seasonal budgets of reactive nitrogen species and ozone over the United States, and export fluxes to the global atmosphere." *Journal of Geophysical Research-Atmospheres*, 103(D11), 13435-13450.
- Lopez-Hilfiker, F. D., Mohr, C., Ehn, M., Rubach, F., Kleist, E., Wildt, J., Mentel, T. F., Carrasquillo, A. J., Daumit, K. E., Hunter, J. F., Kroll, J. H., Worsnop, D. R., and Thornton, J. A. (2015). "Phase partitioning and volatility of secondary organic aerosol components formed from alpha-pinene ozonolysis and OH oxidation: the importance

- of accretion products and other low volatility compounds." *Atmospheric Chemistry and Physics*, 15(14), 7765-7776.
- Lopez-Hilfiker, F. D., Mohr, C., Ehn, M., Rubach, F., Kleist, E., Wildt, J., Mentel, T. F., Lutz, A., Hallquist, M., Worsnop, D., and Thornton, J. A. (2014). "A novel method for online analysis of gas and particle composition: description and evaluation of a Filter Inlet for Gases and AEROSols (FIGAERO)." *Atmospheric Measurement Techniques*, 7(4), 983-1001.
- Loreto, F., Dicke, M., Schnitzler, J. P., and Turlings, T. C. J. (2014). "Plant volatiles and the environment." *Plant Cell and Environment*, 37(8), 1905-1908.
- Maksymiuk, C. S., Gayahtri, C., Gil, R. R., and Donahue, N. M. (2009). "Secondary organic aerosol formation from multiphase oxidation of limonene by ozone: mechanistic constraints via two-dimensional heteronuclear NMR spectroscopy." *Physical Chemistry Chemical Physics*, 11(36), 7810-7818.
- Mohr, C., Lopez-Hilfiker, F. D., Yli-Juuti, T., Heitto, A., Lutz, A., Hallquist, M., D'Ambro, E. L., Rissanen, M. P., Hao, L. Q., Schobesberger, S., Kulmala, M., Mauldin, R. L., Makkonen, U., Sipila, M., Petaja, T., and Thornton, J. A. (2017). "Ambient observations of dimers from terpene oxidation in the gas phase: Implications for new particle formation and growth." *Geophysical Research Letters*, 44(6), 2958-2966.
- Mutzel, A., Poulain, L., Berndt, T., Iinuma, Y., Rodigast, M., Böge, O., Richters, S., Spindler, G., Sipilä, M., Jokinen, T., Kulmala, M., and Herrmann, H. (2015). "Highly Oxidized Multifunctional Organic Compounds Observed in Tropospheric Particles: A Field and Laboratory Study." *Environmental Science & Technology*, 49(13), 7754-7761.
- Myrdal, P. B., and Yalkowsky, S. H. (1997). "Estimating pure component vapor pressures of complex organic molecules." *Industrial & Engineering Chemistry Research*, 36(6), 2494-2499.
- Nannoolal, Y., Rarey, J., and Ramjugernath, D. (2008). "Estimation of pure component properties - Part 3. Estimation of the vapor pressure of non-electrolyte organic compounds via group contributions and group interactions." *Fluid Phase Equilibria*, 269(1-2), 117-133.
- Nannoolal, Y., Rarey, J., Ramjugernath, D., and Cordes, W. (2004). "Estimation of pure component properties Part 1. Estimation of the normal boiling point of non-electrolyte organic compounds via group contributions and group interactions." *Fluid Phase Equilibria*, 226, 45-63.
- Ng, N. L., Chhabra, P. S., Chan, A. W. H., Surratt, J. D., Kroll, J. H., Kwan, A. J., McCabe, D. C., Wennberg, P. O., Sorooshian, A., Murphy, S. M., Dalleska, N. F., Flagan, R. C., and Seinfeld, J. H. (2007). "Effect of NO_x level on secondary organic aerosol (SOA) formation from the photooxidation of terpenes." *Atmos. Chem. Phys.*, 7(19), 5159-5174.
- Nguyen, T. L., Peeters, J., and Vereecken, L. (2009). "Theoretical study of the gas-phase ozonolysis of beta-pinene (C₁₀H₁₆)." *Physical Chemistry Chemical Physics*, 11(27), 5643-5656.

- Niinemets, U. (2010). "Mild versus severe stress and BVOCs: thresholds, priming and consequences." *Trends in Plant Science*, 15(3), 145-153.
- Pankow, J. F. (1994). "An absorption model of the gas/aerosol partitioning involved in the formation of secondary organic aerosol." *Atmospheric Environment*, 28(2), 189-193.
- Pathak, R. K., Salo, K., Emanuelsson, E. U., Cai, C. L., Lutz, A., Hallquist, A. M., and Hallquist, M. (2012). "Influence of Ozone and Radical Chemistry on Limonene Organic Aerosol Production and Thermal Characteristics." *Environmental Science & Technology*, 46(21), 11660-11669.
- Riva, M., Heikkinen, L., Bell, D. M., Peräkylä, O., Zha, Q., Schallhart, S., Rissanen, M. P., Imre, D., Petäjä, T., Thornton, J. A., Zelenyuk, A., and Ehn, M. (2019). "Chemical transformations in monoterpene-derived organic aerosol enhanced by inorganic composition." *npj Climate and Atmospheric Science*, 2(1), 2.
- Salo, K., Hallquist, M., Jonsson, A. M., Saathoff, H., Naumann, K. H., Spindler, C., Tillmann, R., Fuchs, H., Bohn, B., Rubach, F., Mentel, T. F., Müller, L., Reinnig, M., Hoffmann, T., and Donahue, N. M. (2011). "Volatility of secondary organic aerosol during OH radical induced ageing." *Atmospheric Chemistry and Physics*, 11(21), 11055-11067.
- Salo, K., Jonsson, A. M., Andersson, P. U., and Hallquist, M. (2010). "Aerosol Volatility and Enthalpy of Sublimation of Carboxylic Acids." *Journal of Physical Chemistry A*, 114(13), 4586-4594.
- Sanchez, J., Tanner, D. J., Chen, D. X., Huey, L. G., and Ng, N. L. (2016). "A new technique for the direct detection of HO₂ radicals using bromide chemical ionization mass spectrometry (Br-CIMS): initial characterization." *Atmospheric Measurement Techniques*, 9(8), 3851-3861.
- Shiraiwa, M., Ueda, K., Pozzer, A., Lammel, G., Kampf, C. J., Fushimi, A., Enami, S., Arangio, A. M., Fröhlich-Nowoisky, J., Fujitani, Y., Furuyama, A., Lakey, P. S. J., Lelieveld, J., Lucas, K., Morino, Y., Pöschl, U., Takahama, S., Takami, A., Tong, H., Weber, B., Yoshino, A., and Sato, K. (2017). "Aerosol Health Effects from Molecular to Global Scales." *Environmental Science & Technology*, 51(23), 13545-13567.
- Shrivastava, M., Cappa, C. D., Fan, J. W., Goldstein, A. H., Guenther, A. B., Jimenez, J. L., Kuang, C., Laskin, A., Martin, S. T., Ng, N. L., Petaja, T., Pierce, J. R., Rasch, P. J., Roldin, P., Seinfeld, J. H., Shilling, J., Smith, J. N., Thornton, J. A., Volkamer, R., Wang, J., Worsnop, D. R., Zaveri, R. A., Zelenyuk, A., and Zhang, Q. (2017). "Recent advances in understanding secondary organic aerosol: Implications for global climate forcing." *Reviews of Geophysics*, 55(2), 509-559.
- Stocker, T. F., D. Qin, G.-K. Plattner, M. Tignor, S.K. Allen, J. Boschung, A. Nauels, Y. Xia, V. Bex and P.M. Midgley (eds.). (2013). *IPCC, 2013: Climate Change 2013: The Physical Science Basis. Contribution of Working Group I to the Fifth Assessment Report of the Intergovernmental Panel on Climate Change*
- Trostl, J., Chuang, W. K., Gordon, H., Heinritzi, M., Yan, C., Molteni, U., Ahlm, L., Frege, C., Bianchi, F., Wagner, R., Simon, M., Lehtipalo, K., Williamson, C., Craven, J. S., Duplissy, J., Adamov, A., Almeida, J., Bernhammer, A. K., Breitenlechner, M., Brilke, S., Dias, A., Ehrhart, S., Flagan, R. C., Franchin, A., Fuchs, C., Guida, R.,

- Gysel, M., Hansel, A., Hoyle, C. R., Jokinen, T., Junninen, H., Kangasluoma, J., Keskinen, H., Kim, J., Krapf, M., Kurten, A., Laaksonen, A., Lawler, M., Leiminger, M., Mathot, S., Mohler, O., Nieminen, T., Onnela, A., Petaja, T., Piel, F. M., Miettinen, P., Rissanen, M. P., Rondo, L., Sarnela, N., Schobesberger, S., Sengupta, K., Sipila, M., Smith, J. N., Steiner, G., Tome, A., Virtanen, A., Wagner, A. C., Weingartner, E., Wimmer, D., Winkler, P. M., Ye, P. L., Carslaw, K. S., Curtius, J., Dommen, J., Kirkby, J., Kulmala, M., Riipinen, I., Worsnop, D. R., Donahue, N. M., and Baltensperger, U. (2016). "The role of low-volatility organic compounds in initial particle growth in the atmosphere." *Nature*, 533(7604), 527-+.
- Tsigaridis, K., Daskalakis, N., Kanakidou, M., Adams, P. J., Artaxo, P., Bahadur, R., Balkanski, Y., Bauer, S. E., Bellouin, N., Benedetti, A., Bergman, T., Berntsen, T. K., Beukes, J. P., Bian, H., Carslaw, K. S., Chin, M., Curci, G., Diehl, T., Easter, R. C., Ghan, S. J., Gong, S. L., Hodzic, A., Hoyle, C. R., Iversen, T., Jathar, S., Jimenez, J. L., Kaiser, J. W., Kirkevag, A., Koch, D., Kokkola, H., Lee, Y. H., Lin, G., Liu, X., Luo, G., Ma, X., Mann, G. W., Mihalopoulos, N., Morcrette, J. J., Muller, J. F., Myhre, G., Myriokefalitakis, S., Ng, N. L., O'Donnell, D., Penner, J. E., Pozzoli, L., Pringle, K. J., Russell, L. M., Schulz, M., Sciare, J., Seland, O., Shindell, D. T., Sillman, S., Skeie, R. B., Spracklen, D., Stavrou, T., Steenrod, S. D., Takemura, T., Tiitta, P., Tilmes, S., Tost, H., van Noije, T., van Zyl, P. G., von Salzen, K., Yu, F., Wang, Z., Wang, Z., Zaveri, R. A., Zhang, H., Zhang, K., Zhang, Q., and Zhang, X. (2014). "The AeroCom evaluation and intercomparison of organic aerosol in global models." *Atmospheric Chemistry and Physics*, 14(19), 10845-10895.
- Tsigaridis, K., and Kanakidou, M. (2007). "Secondary organic aerosol importance in the future atmosphere." *Atmospheric Environment*, 41(22), 4682-4692.
- Tu, P. J., Hall, W. A., and Johnston, M. V. (2016). "Characterization of Highly Oxidized Molecules in Fresh and Aged Biogenic Secondary Organic Aerosol." *Analytical Chemistry*, 88(8), 4495-4501.
- Vereecken, L., and Francisco, J. S. (2012). "Theoretical studies of atmospheric reaction mechanisms in the troposphere." *Chemical Society Reviews*, 41(19), 6259-6293.
- Veres, P., Roberts, J. M., Warneke, C., Welsh-Bon, D., Zahniser, M., Herndon, S., Fall, R., and de Gouw, J. (2008). "Development of negative-ion proton-transfer chemical-ionization mass spectrometry (NI-PT-CIMS) for the measurement of gas-phase organic acids in the atmosphere." *International Journal of Mass Spectrometry*, 274(1-3), 48-55.
- Winterhalter, R., Neeb, P., Grossmann, D., Kolloff, A., Horie, O., and Moortgat, G. (2000). "Products and mechanism of the gas phase reaction of ozone with beta-pinene." *Journal of Atmospheric Chemistry*, 35(2), 165-197.
- Virtanen, A., Joutsensaari, J., Koop, T., Kannosto, J., Yli-Pirila, P., Leskinen, J., Makela, J. M., Holopainen, J. K., Poschl, U., Kulmala, M., Worsnop, D. R., and Laaksonen, A. (2010). "An amorphous solid state of biogenic secondary organic aerosol particles." *Nature*, 467(7317), 824-827.
- Volkamer, R., Jimenez, J. L., San Martini, F., Dzepina, K., Zhang, Q., Salcedo, D., Molina, L. T., Worsnop, D. R., and Molina, M. J. (2006). "Secondary organic aerosol formation

from anthropogenic air pollution: Rapid and higher than expected." *Geophysical Research Letters*, 33(17), 4.

- Xu, L., Guo, H. Y., Boyd, C. M., Klein, M., Bougiatioti, A., Cerully, K. M., Hite, J. R., Isaacman-VanWertz, G., Kreisberg, N. M., Knote, C., Olson, K., Koss, A., Goldstein, A. H., Hering, S. V., de Gouw, J., Baumann, K., Lee, S. H., Nenes, A., Weber, R. J., and Ng, N. L. (2015). "Effects of anthropogenic emissions on aerosol formation from isoprene and monoterpenes in the southeastern United States." *Proceedings of the National Academy of Sciences of the United States of America*, 112(1), 37-42.
- Yatawelli, R. L. N., Stark, H., Thompson, S. L., Kimmel, J. R., Cubison, M. J., Day, D. A., Campuzano-Jost, P., Palm, B. B., Hodzic, A., Thornton, J. A., Jayne, J. T., Worsnop, D. R., and Jimenez, J. L. (2014). "Semicontinuous measurements of gas-particle partitioning of organic acids in a ponderosa pine forest using a MOVI-HRToF-CIMS." *Atmospheric Chemistry and Physics*, 14(3), 1527-1546.
- Zhang, D., and Zhang, R. (2005). "Ozonolysis of alpha-pinene and beta-pinene: Kinetics and mechanism." *Journal of Chemical Physics*, 122(11), 12.
- Zhang, X., Lambe, A. T., Upshur, M. A., Brooks, W. A., Be, A. G., Thomson, R. J., Geiger, F. M., Surratt, J. D., Zhang, Z. F., Gold, A., Graf, S., Cubison, M. J., Groessl, M., Jayne, J. T., Worsnop, D. R., and Canagaratna, M. R. (2017). "Highly Oxygenated Multifunctional Compounds in alpha-Pinene Secondary Organic Aerosol." *Environmental Science & Technology*, 51(11), 5932-5940.
- Zhang, Y. Y., Muller, L., Winterhalter, R., Moortgat, G. K., Hoffmann, T., and Poschl, U. (2010). "Seasonal cycle and temperature dependence of pinene oxidation products, dicarboxylic acids and nitrophenols in fine and coarse air particulate matter." *Atmospheric Chemistry and Physics*, 10(16), 7859-7873.